UNIVERSITY OF TARTU

FACULTY OF SCIENCE AND TECHNOLOGY

Institute of Chemistry

Shanshan Wu

# Optimization of ARC-Lum Based Time-Gated Photoluminescence Method for Determination of Affinities of Protein Kinase Inhibitors

Master's Thesis

Supervisors: Hedi Sinijärv, MSc

Asko Uri, PhD

Tartu 2014

# Abbreviations

ARC – adenosine analogue-oligoarginine conjugate

ATP – adenosine-5’-triphosphate

BSA – bovine serum albumin

cAMP – 3'-5'-cyclic adenosine monophosphate

DDT – dithiothreitol, (*2S,3S*)-1,4-bis(sulfanyl)butane-2,3-diol

FRET – Förster resonance energy transfer

HEPES – 4-(2-hydroxyethyl)-1-piperazineethanesulfonic acid

HTS – high-throughput screening

$IC_{50}$ – half-maximal inhibitory concentration

$K_D$ – dissociation equilibrium constant in direct binding assay

$K_d$ – dissociation equilibrium constant in displacement assay

PKA – cAMP-dependent protein kinase

PKAc – catalytic subunit of the cAMP-dependent protein kinase

SD – standard deviation

TGL – time-gated luminescence

TR-FRET – time-gated FRET

UV-Vis – ultraviolet-visible

Z-factor – screening window coefficient

$\varepsilon$ – molar extinction coefficient

# Table of Contents

# 1. Introduction

Measurements of biochemical analytes are often difficult due to complicated matrixes and instability of substances. Nevertheless, these analyses are important for the development of biomedical research tools and drugs.

The disadvantageous aberrant activity of protein kinases has triggered an increasing need for reliable methods for characterizing the inhibitors of protein kinases. In the medicinal chemistry research group at the Institute of Chemistry of University of Tartu different variety of bisubstrate inhibitors called ARCs for protein kinases have been developed. Based on ARCs novel photoluminescent probes have been constructed that have found applications in screening and characterization of kinases, but also in methods for evaluating the affinity of new inhibitors.

Time-resolved photoluminescence method based on the application of ARC-Lum probes is a high-throughput screening assay that combines several advantages of using Förster resonance energy transfer induced signal amplification together with time gated measurements. This method can be used to determine the affinity of protein kinase inhibitors that bind to the binding sites of ATP and/or substrate. The responsiveness of the luminescence signal to the presence of the target protein enables the realization of the assays in biological matrixes without any significant interference.

The purpose of this work was to determine the optimal conditions for ARC-Lum based time-resolved photo-luminescence method for affinity analysis of inhibitors with different properties.

# 2. Literature Overview

## 2.1. Protein Kinases

Protein kinases catalyze the transfer of the γ-phosphoryl group from adenosine-5'-triphosphate (ATP) to a serine, threonine or tyrosine residue of a protein substrate. With this simple chemical reaction, the structure of a protein substrate is modified and consequently, the intercellular communication is affected. The latter, in turn, is related to physiological responses, like homeostasis, function of the nervous and immune system (Manning *et al.* 2002). However, the aberrant activity of protein kinases is related to many human diseases, for instance cancer, diabetes, rheumatoid arthritis, hypertension, schizophrenia and obesity (Hanks & Hunter 1995, Manning et al. 2002).

There was a prediction made about 27 years ago that the human genome includes 1001 protein kinases (Hunter 1987) and five years later even a larger number was proposed (Hunter 1994). Since then, the scientists have made remarkable contributions to identify all of the human protein kinases. In 1988, approximately 100 protein kinases had been identified (Hanks *et al.* 1988). The number reached 538 in 2011, constituting about 2% of 23000 human genes (Schwartz & Murray 2011). Protein kinases are classified into eight main groups, based on the amino acid sequence similarity of the catalytic domain. (Hanks & Hunter 1995, Manning et al. 2002).

A thoroughly examined protein kinase, the cAMP-dependent protein kinase (PKA) from AGC group, was identified in 1968 (Walsh *et al.* 1968). PKA is a serine/threonine-specific kinase, omnipresent in human cells, that is responsible for enforcement of a large number of intracellular signaling events. At its inactive state PKA is a heterotetrameric holoenzyme that comprises a regulatory subunit dimer and two catalytic subunits (PKAc) (Krebs & Beavo 1979). The binding of 2 molecules of 3'-5'-cyclic adenosine monophosphate (cAMP), which is an important second messenger in the cell, to a regulatory subunit leads to a conformational change of the protein complex. Consequently, the PKA holenzyme is dissociated into a regulatory subunit dimer and two active catalytic subunits, PKAc (Anand *et al.* 2010, Kim *et al.* 2005, Sjoberg *et al.* 2010).

Despite of the importance of protein kinases in cell life, only a very small portion of them are targeted with the drugs that have reached the clinic (Schwartz & Murray 2011). The reason for

that lies in the problem that the role of many protein kinases in cell life has not been established yet (Fedorov *et al.* 2010). For this reason, there is a high need for reliable methods and well characterized inhibitors and probes that would enable tracking the localization and regulation the activity of protein kinases in cells.

## 2.2. Inhibitors of Protein Kinases

As mentioned before, protein kinases regulate a large number of cellular processes, and the over-expressed kinases have pathological consequences. To solve this problem, the field of drug development activities related to inhibitors of protein kinases is constantly increasing. Among all types of the inhibitors of protein kinases, including antibodies, small molecule inhibitors have been preferably chosen for drug research as they inhibit the abnormal activity of protein kinases directly. Although the majority of mentioned studies are focused on oncology, more and more clinical trials have been carried out for the treatment of other diseases, for example, the treatment of inflammatory diseases (Cohen & Alessi 2013).

The selective inhibitors with suitable optical properties can also be used as probes to study different intracellular and extracellular enzymes (Cravatt *et al.* 2008), *e.g.* for the determination of activity and location of protein kinases (Kasari *et al.* 2012, Vaasa *et al.* 2012). Furthermore, such probes can also be used to characterize the irreversible inhibitors (Barf & Kaptein 2012).

There are some general requirements for an ideal inhibitor, either it is used as a probe or as a potential drug. First, the inhibitors should block substrate binding sites of protein kinases. Second, inhibitors should have a good selectivity. At last, they should have high bioavailability and low toxicity (Parang & Cole 2002).

According to the inhibitor's targeting site at the catalytic domain of protein kinase, the inhibitors can be classified into four types: ATP-competitive inhibitors, protein/peptide-competitive inhibitors, bisubstrate inhibitors and allosteric inhibitors (Bogoyevitch & Fairlie 2007).

### 2.2.1. ATP-Competitive Inhibitors

ATP-competitive inhibitor is an inhibitor which inhibits the protein kinase by targeting the ATP-site of the catalytic domain (Bridges 2001, Lawrence & Niu 1998, Lindsley *et al.* 2007). Although the majority of protein kinase inhibitors that have been characterized belong to this group, the development of small and selective ATP-site inhibitors faces two major challenges:

selectivity and potency. It has been challenging to develop kinase inhibitors that can inhibit only one of the 538 protein kinases which have rather similar ATP-binding pockets (Bain *et al.* 2003, Bain *et al.* 2007, Davies *et al.* 2000). Furthermore, the inhibitor, which targets the ATP-binding site of the kinase, needs to have a sufficient potency to compete with the high (millimolar) concentration of ATP present in the cell (Gribble *et al.* 2000).

Nevertheless, a number of ATP-competitive protein kinase inhibitors have been approved by U.S. Food and Drug Administration, for example: erlotinib, gefitinib and imatinib (Kondapalli *et al.* 2005). The latter, for example, has high inhibitory potency towards a limited number of kinases and thus can be used for the treatment of chronic myelogenous leukemia, gastrointestinal tumors and myeloproliferative diseases (Cohen & Alessi 2013).

### 2.2.2. Protein/Peptide-Competitive Inhibitors

As the binding sites of protein/peptide substrates differ from kinase to kinase, the protein/peptide-competitive inhibitors have relatively higher selectivity compared to ATP-competitive inhibitors (Bogoyevitch *et al.* 2005). Furthermore, the affinity of protein/peptide-competitive inhibitors is enhanced at a high concentration of ATP due to the positive cooperativity when the ATP-site is occupied (Masterson *et al.* 2008).

One of the disadvantages that protein/peptide-competitive inhibitors often possess is the low stability of the compounds due to the presence of proteases in the cellular environment. Furthermore, peptide-based protein substrate-competitive inhibitors are longer structures in order to achieve high inhibitory potency (Bogoyevitch et al. 2005). This, on the other hand, may cause problems of absorption, distribution and toxicity (Zhao & Tang 2007). Fortunately, the "hot-spot" theory solved this problem. This theory revealed that only small number of peptide residues contribute to the binding energy (London *et al.* 2010, Bogan & Thorn 1998). This was a discovery that enhanced the development of small molecule substrate protein/peptide-competitive inhibitors.

### 2.2.3. Bisubstrate Inhibitors

Bisubstrate inhibitor, just as its name implies, is an inhibitor, which inhibits protein kinases by blocking the binding sites of ATP and protein/peptide simultaneously. It aims to overcome the common shortcomings of ATP and protein/peptide-competitive inhibitors (Hines & Cole 2004, Lavogina et al. 2010, Parang & Cole 2002, Parang *et al.* 2001, Ricouart *et al.* 1991, Schneider

*et al.* 2005). However, bisubstrate inhibitors also combine some drawbacks of these two type of inhibitors such as high molecular mass, which results in low bioavailability, and low stability of the peptide moieties (Lavogina et al. 2010). The latter problems can be solved by incorporating structure elements that can improve the cell plasma membrane penetration properties and proteolytic stability (Kayser *et al.* 2007, Kayser-Bricker *et al.* 2009).

#### 2.2.3.1. Adenosine Analogue-Oligoarginine Conjugates

According to the requirements for bisubstrate inhibitors, the medicinal chemistry research group of the Institute of Chemistry (University of Tartu) has developed several compounds called the adenosine analogue-oligoarginine conjugates (ARCs) (Loog *et al.* 1999). The adenosine mimic, targeting the ATP-binding site, and the arginine-rich peptide, targeting the protein/peptide-binding site, are joined together with a flexible linker (Figure 1.).

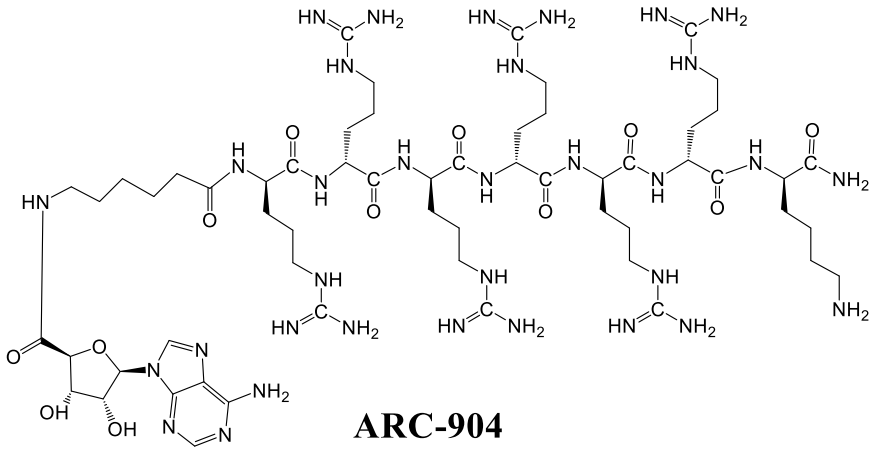


**Figure 1.** An example of an ARC-based inhibitor (Vaasa *et al.* 2009)

During 15 years, different generations of ARCs have been developed, mainly for inhibiting the basophilic protein kinases. When the first ARCs contained L-arginines, a 6-aminohexanoic acid as a linker and had sub-micromolar affinity towards PKAc (Enkvist *et al.* 2006, Loog et al. 1999), then the latest ARCs include D-amino acid residues, two linkers with a chiral spacer, possess picomolar affinities and enhanced proteolytic stability (Lavogina et al. 2010, Lavogina *et al.* 2009, Vaasa et al. 2009). A number of ARCs have been labeled with a fluorescent dye, which enables to use them as optical probes in different applications: *e.g.* testing of new compounds towards biologically important targets like protein kinases (Vaasa et al. 2009), mapping of protein kinases in living cells (Vaasa *et al.* 2010). Fluorescently labeled ARCs containing a thiophene or a selenophene moiety were introduced in 2011 (Enkvist *et al.* 2011).

These ARC-Lum probes have the unique property to give long-lifetime luminescence emission when bound to protein kinases. The discovery of this phenomenon expanded the applications of ARCs even more (Kasari *et al.* 2013, Vaasa et al. 2012).

## 2.3. Luminescence-Based Methods for Characterizing Inhibitors

Characterization of inhibitors of protein kinases is of crucial importance for the development of biomedical research tools and drugs. Consequently, the need for reliable high-throughput screening (HTS) methods is continuously increasing.

Inhibition of enzymatic phosphorylation, homogeneous direct binding and displacement assays are the most frequently used methods for characterization of inhibitors of protein kinases. In the inhibition assay, the velocity of product formation or the final concentration of the product is observed with and without the presence of the inhibitor (Kuznetsov *et al.* 2004). However, inhibition assays require at least both donor (ATP) and acceptor (peptide substrate) of phosphoryl group. In some assay setups, radioactively labeled phosphoryl group is used, which is hazardous to humans and the environment.

In contrast, the homogeneous direct binding or displacement assay formats do not require phosphoryl group donor and acceptor. Instead, a fluorescently labeled inhibitor (a probe) could be used (Viht *et al.* 2005). The signal emitted by the probe is different if it is free or bound to the kinase. In case of direct binding assay, the labeled compound is characterized by observing the binding to the protein kinases directly (Vaasa et al. 2009). The displacement binding, on the other hand, is usually applied for the determination of properties of unlabeled inhibitors by displacing the labeled probe from the complex with a protein kinase (Enkvist *et al.* 2012). Due to the low consumption of reagents, high sensitivity and applicability in HTS, luminescence is becoming a dominant technique used in binding assays (Uri *et al.* 2010).

### 2.3.1. Principles of Photoluminescence

The light emitted from electronically excited states by substances is called luminescence. There are two subtypes of luminescence differenced by the nature of the excited state – phosphorescence and fluorescence (Figure 2). When a rigid molecule absorbs electromagnetic radiation (UV radiation or light), an electron is excited from the ground singlet state ($S_0$) to a higher singlet state ($S_1$ or $S_2$). After that, the excited electron rapidly returns to the lowest vibrational level of $S_1$. This is called an internal conversion, which is a non-radiative process.

In a case of some molecules, if an electron reaches to the ground state, fluorescence is emitted during ~$10^{-8}$ seconds (Lakowicz 2006). In case of phosphorescence, after the absorption of electromagnetic radiation and excitement of the electron, the latter is transited from $S_1$ to the first triplet state ($T_1$) through singlet-triplet intersystem crossing. During the relaxation from $T_1$ to $S_0$, phosphorescence with a considerably longer lifetime (approximately milliseconds) is emitted.

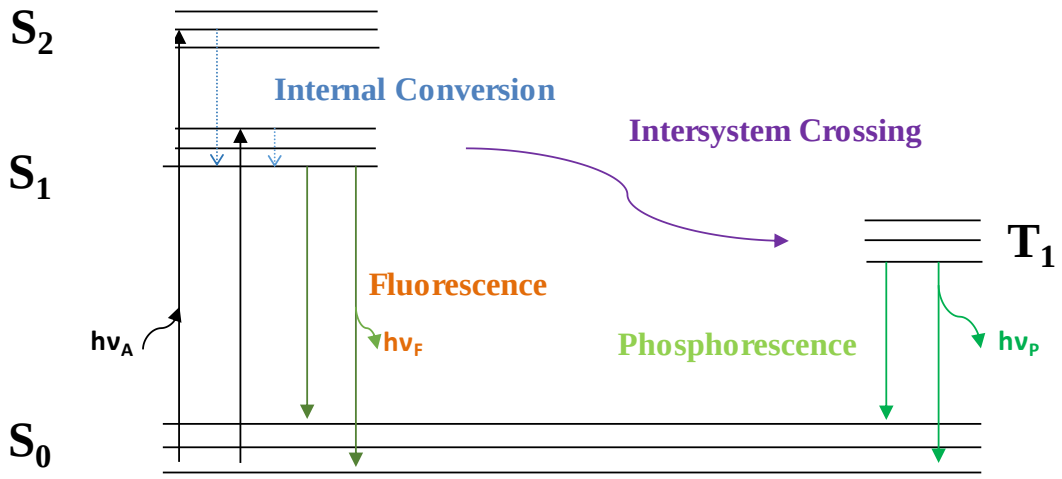


**Figure 2.** Principles of fluorescence and phosphorescence. $S_0$, $S_1$, $S_2$ and $T_1$ denote as the singlet ground, first electronic state, second electronic state and first triplet state, respectively (Lakowicz 2006).

Based on the principles of fluorescence and phosphorescence four measurement methods are introduced: fluorescence anisotropy (FA), time-gated luminescence (TGL), Förster resonance energy transfer (FRET), and time-resolved FRET (TR-FRET)[1].

### 2.3.2. Fluorescence Anisotropy

FA assay enables the investigation of interactions between molecules, *e.g.* a probe and a kinase (Ehrlich *et al.* 2011). In FA assay the sample is excited by a linearly polarized light. For detection, the emitted light is directed through a parallel and a perpendicular polarizer (with respect to the incident light). Accordingly, the equation of FA is defined (Equation 1).

[1] Although "time-gated" and "time-resolved" have a similar meaning, the first is usually used together with the term "luminescence", and the latter with "FRET".

$$FA = \frac{I_{\text{II}} - I_{\perp}}{I_{\text{II}} + 2I_{\perp}}$$

**Equation 1**. Fluorescence anisotropy equation (Lakowicz 2006). $I_{\text{II}}$ and $I_{\perp}$ are parallel and perpendicularly polarized fluorescence intensities, respectively, in the condition where the sample is excited with vertically incident light.

Due to the small molecular weight (usually less than 3 kDa), the free fluorescence probe rotates several times within the fluorescence lifetime of a fluorophore (Lakowicz 2006). This results in depolarization of the emitted light, giving roughly the same intensities in both of the angular directions and therefore a small value for fluorescence anisotropy (Lakowicz 2006). If the probe-kinase complex is formed, the rotational tumbling of the fluorophore is reduced as the kinase (MW >30 kDa) has substantially longer rotational correlation time. Slower rotation of the fluorophore due to the binding causes the $I_{\text{II}}$ to increase and $I_{\perp}$ to decrease, resulting in higher value of fluorescence anisotropy.

Although fluorescence anisotropy is a powerful method often used in the biological and biophysical fields (Ehrlich *et al*. 2011), there are two disadvantages. First, one has to be cautious using this method with complicated solutions, *e.g.* containing non-target proteins at high concentrations (cell lysates, bodily fluids). For example, there might be non-specific binding of the probe to other components, which results in nonspecific anisotropy increase. Additionally, if a low-affinity probe is used in displacement assays, a high concentration of the kinase is needed, which is costly. The higher concentration of the protein kinase guarantees that most of the molecules of the probe are bound to the protein kinase. Otherwise, the free probe would interfere with the polarization measurements. This, on the other hand, influences the reliability of the assay window and the determined affinity.

### 2.3.3. Time-Gated Measurements

FRET, a phenomenon, which was described by Theodor Förster in 1946, is an energy transfer between two fluorescent molecules which occurs if the excitation spectrum of the acceptor chromophore overlaps with the emission spectrum of the donor fluorophore (Förster 1946). If these two chromophores are close enough (1-10 nm) (Figure 3), the excitation of the donor at the lower wavelength energy source triggers the energy transfer to the acceptor, which results in the enhanced emission at the higher wavelength of the acceptor (Arai & Nagai 2013). Because of the requirement close distance between the donor and the acceptor fluorophores for efficient energy transfer, FRET-based assays are sensitive towards interactions of two

molecules, fast and applicable in different fields of , *e.g.* to study protein-protein interactions or to detect nucleic acids (Reischl *et al.* 2003, Li *et al.* 2008). However, the method is sensitive towards the substances present in biological samples that might cause background fluorescence (Riddle *et al.* 2006).

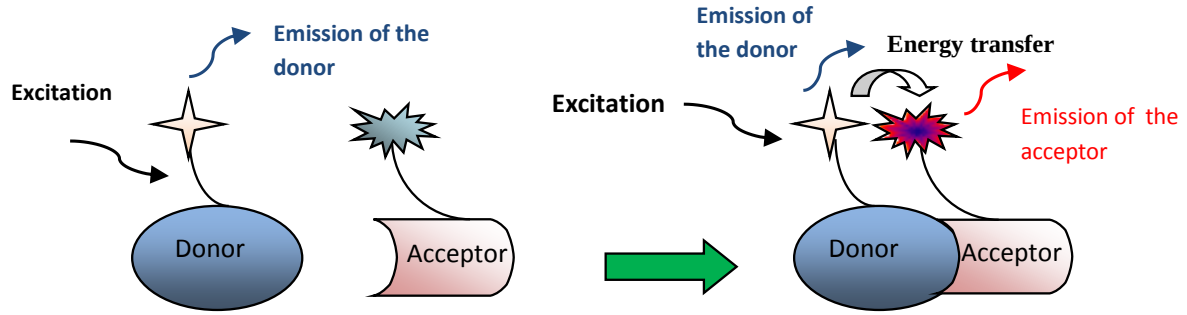


**Figure 3.** The principle of FRET (Sourjik & Berg 2002).

In order to overcome the problems, the combination of time-resolved methods and FRET has been widely used since it was first introduced (Mathis 1995). The main characteristic of time-resolved detection method is a time delay between the excitation pulse and measurement window (Figure 4). The latter is possible, because the donor emits a long lifetime luminescence signal after excitation. Short lifetime and non-specific signal from other compounds in the solution will fade within the delay time.

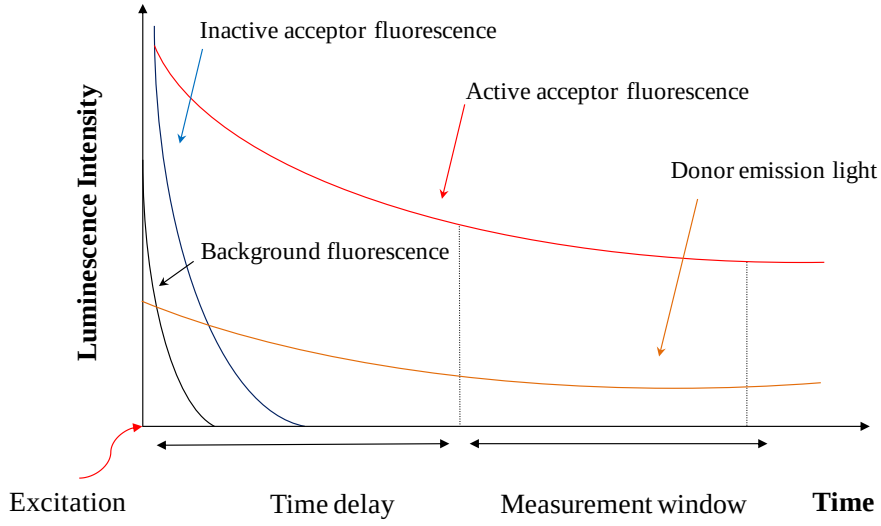


**Figure 4.** Principle of TR-FRET based assay (Enkvist et al. 2011).

Europium and terbium chelates  lanthanides complexes that were first used as long-lifetime luminescence donors (Mathis 1993). Both complexes have very long luminescence half-lives (300 µs to 1 ms) (Bazin *et al.* 2001).

Although the employment of these probes has found successful applications (Lebakken *et al.* 2009), for example in the analysis of protein kinase inhibitors, the need for several compounds for detection reduces the robustness and simplicity of the method. Despite many advantages, lanthanide-based donors have complex structures that badly penetrate cell plasma membrane and may be degraded in biological solutions (Didier *et al.* 2011).

### 2.3.4. ARC-Lum Based TR-FRET Assay

The novel ARC-Lum compounds, introduced in chapter 2.2.3.1, could be used as counterparts of the lanthanide-based probes. The thiophene- or selenophene-containing moiety that binds to the ATP-site of a protein kinase serves as the luminescence donor in the ARC-Lum probe (Enkvist et al. 2011) (Figure 5). Due to the fluorescent label attached to the peptide moiety of the probe, FRET is observed between the excited thiophene/selenophene fragment (a donor) and the fluorophore (an acceptor) with luminescence half-life in the range of 20 - 270 µs This kind of organic molecule possessing intrinsic property of inducing TR-FRET in special conditions is rarely encountered.

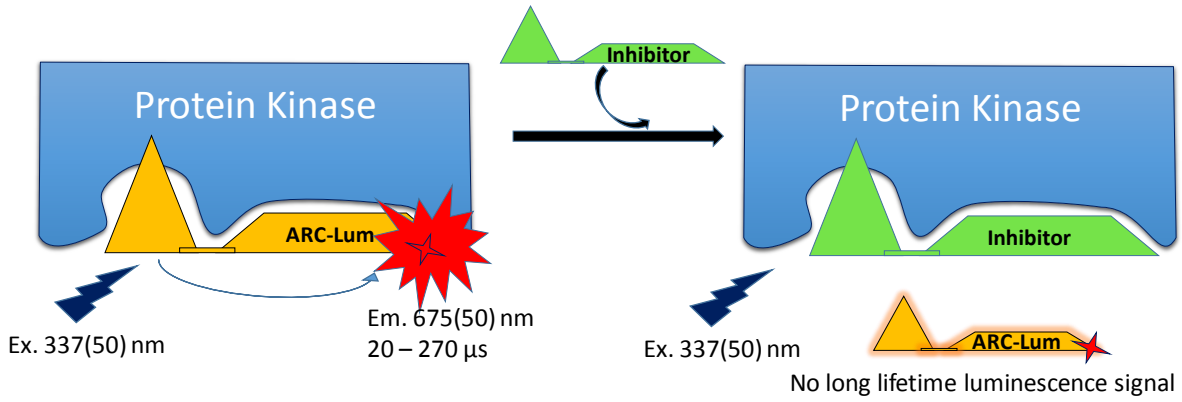


**Figure 5.** Principle of ARC-Lum based TGL Assay. If the sample is irradiated at ~337 nm, the long lifetime luminescence signal at ~675 nm is produced only if the ARC-Lum probe is in complex with a kinase (Kasari et al. 2012). Because of the bisubstrate character ARC-Lum probes they are displaced from the complex with compounds binding to any domain of the active site of the enzyme.

Responsiveness of the ARC-Lum probe is one of the main features to highlight, meaning that the probe will only emit the long-lifetime luminescence if in a complex with a kinase. This is

most probably due to the fixation of the thiophene/selenophene fragment and its effective burial from quenching molecular species and motional effects if positioned in the active site of the protein kinase. Free probe, on the other hand does not emit long-lifetime luminescence. This property can be thus used as an indication whether the probe has bound to the protein kinase or not.

Secondly, ARC-Lum probes have both fluorescent and phosphorescent properties, thus these probes can be used in parallel for fluorescence anisotropy/polarization and TGL assays. Thirdly, ARC-Lum probes can be used displacement assays even when the analyte is an inhibitor with very high affinity. High concentrations of the probe can be used to shift the displacement curve from the tight-binding region as the free probe lacks luminescence signal and there is no significant background noise. What is more, some ARC-Lum probes possess very high affinity (~20 pM) towards PKAc, which enables lowering of its the concentrations and volumes used in the assays. (Kasari et al. 2013, Enkvist et al. 2011)

### 2.3.5. The Affinity Characterization for Inhibitor/Ligand

All of the previously described methods can be used to describe the interactions between an enzyme (*e.g.* protein kinase) and a ligand (*e.g.* an inhibitor). There is a basic interaction of formation of the complex between the free enzyme and free ligand in equilibrium conditions (Equation 2).

$$E + L \underset{k_{-1}}{\overset{k_{+1}}{\rightleftharpoons}} EL$$

**Equation 2.** Scheme of equilibrium binding. The complex (EL) between the free enzyme (E) and free ligand (L) in equilibrium conditions. $k_{+1}$ and $k_{-1}$ denote the association and dissociation rate constants, respectively.

The equilibrium dissociation constant $K_D$ is defined as the ratio of the concentrations of free enzyme and free ligand to the concentration of the formed complex (Equation 3 A). $K_D$ is used to quantify the affinity of the ligand towards the enzyme in direct binding assay and $K_d$ denotes the displacement dissociation constant (Equation 3 B and 3 C) based on the Cheng-Prusoff equation (Cheng & Prusoff 1973).

A) $K_D = \frac{[E][L]}{[EL]}$ B) $K_d = \frac{IC_{50}}{1+\frac{[L]}{K_D}}$ C) $K_d = \frac{IC_{50}}{1+\frac{[L]_{50}}{K_D}+\frac{[P]_0}{K_D}}$

**Equation 3.** A) Equilibrium dissociation constant, ($K_D$), where [E] is the total concentration of the enzyme, [L] is the total concentration of the ligand and [EL] the concentration of the complex; B) equilibrium dissociation constant ($K_d$) determined from the displacement assay, where $IC_{50}$ refers to the concentration of a competitive inhibitor at the point, where 50% of the ligand is displaced from the ligand-kinase complex; C) equilibrium dissociation constant determined in a displacement assay, taking into account of active concentration of kinase. Where $[L]_{50}$ and $[P]_{50}$ are denoted as the concentration of the free labeled ligand at 50% inhibition and the concentration of the free protein at 0% inhibition respectively (Nikolovska-Coleska et al. 2004).

### 2.3.6. Z-Factor

Z-factor is a screening window coefficient which is used to estimate the assay window range and the data variations (Zhang *et al.* 1999). The Z-factor in displacement assays is defined as (Equation 4):

$$Z = 1 - \frac{3 \times SD \text{ of upper plateau values} + 3 \times SD \text{ of lower plateau values}}{\text{mean of upper plateau values} - \text{mean of lower plateau values}}$$

**Equation 4.** The equation of Z-factor in case of displacement assay. Where the upper plateau indicates the positive control, where the signal is formed, and the lower plateau indicates the negative control, where there should not be any signal.

The range of Z-factor is from 1 to -1. If $Z = 1$, $SD = 0$ or the distance between the upper plateau value and the lower plateau value is infinite, describing an ideal assay. If $1 > Z \geq 0.5$, separation band is large, which describes an excellent assay. If $0.5 > Z \geq 0$, separation band is small and if $Z = 0$, there is no separation band and the upper plateau and the lower plateau are not separated. If Z-factor < 0, there is no separation and the upper plateau value and lower plateau overlap with each other, which is a scenario impossible to be applied in the screening assay. In general, the Z-factor can be used as a parameter to validate the assay procedure, and the instrument. In addition, the Z-factor is also sensitive to assay conditions, for example, the chemical composition and the concentrations (Zhang et al. 1999).

# 3. Experimental

## 3.1. Chemicals and Materials

Chemicals used in the experiments were obtained from the following sources: human PKAc was produced and purified by Taavi Ivan and Jevgenia Bredihhina (Rogozina) University of Tromsø as previously described (Lavogina et al. 2009); bovine serum albumin (BSA), dithiothreitol (DTT), HEPES hemisodium salt and Tween® 20 from Sigma Life Science; sodium chloride from Riedel-de Haën; Bodipy FL from Invitrogen. All the solutions were made in MilliQ water (Millipore Corporation).

The ARCs used in the experiments were ARC-1042, ARC-1182 (ARC-Lum), ARC-1063 (ARC-Lum), ARC-904, ARC-1411 and ARC-1012 (Appendix 1), synthesized in the Asko Uri's research group (Institute of Chemistry, University of Tartu) (Enkvist et al. 2011, Vaasa et al. 2009, Viira 2012).

Assays were performed in the following buffers. 5-component buffer: 50 mM HEPES, 150 mM NaCl, 7.5 µM or 1.5 µM BSA, 5 nM DTT, 0.005% Tween® 20, *pH* = 7.4. 4-component buffer: 50 mM HEPES, 150 mM NaCl, 5 nM DTT, 0.005% Tween® 20, *pH* = 7.4. 3-component buffer: 50 mM HEPES, 150 mM NaCl, 0.005% Tween® 20, *pH* = 7.4.

## 3.2. Equipment

| **Equipment** | **Manufacturer** | **Supplementary information** |
|---|---|---|
| 384-well microplates | Corning | Non-binding surface, code 3676 |
| Centrifuge | Sigma | 3-16 PK; rotor: 11133 |
| Spectrophotometer | Thermo Scientific | NanoDrop 2000c |
| Vortex | IKA | MS 3 basic |
| Microplate shaker-incubator | BMG Labtech | THERMOstar |
| Automatic 8-channel pipette | INTEGRA Biosciences | 5…125 µl |
| Manual Pipette | Eppendorf | 0.1 … 2.5 µl;<br>0.5 … 10 µl;<br>2 … 20 µl;<br>10 … 100 µl;<br>20 … 200 µl;<br>100 … 1000 µl |
| Microplate Reader | BMG Labtech | PHERAstar Plus<br>Detector: Photomultiplier tubes<br>Lamp: Xenon flash lamp |

The following programs were used: Prism 5.0 (Graphpad software), SPSS statistic 19.0 (International Business Machines Corporation), Microsoft Excel 2007 (Microsoft Corporation), NanoDrop2000 (Thermo Scientific), ChemDraw (PerkinElmer Incorporation).

## 3.3. Determination of the Concentrations of ARC-Compounds

Solid ARCs were dissolved in the 3-component buffer. The absorption was measured with a spectrophotometer at absorption maximum of the UV-Vis spectrum for at least 5 times and the average value was used to calculate the concentration of ARC-compounds according to the Beer-Lambert's equation (Equation 5). The extinction coefficients of ARC-compounds are reported in Table 1. The optical path length of the NanoDrop 2000c instrument was 0.10 cm. The concentration of the solutions of ARCs were determined before every series of measurements.

$$A_\lambda = \varepsilon_\lambda l c$$

**Equation 5**. Beer-Lambert's law: $A_\lambda$ – absorption at wavelength $\lambda$, $\varepsilon$ – molar extinction coefficient [$M^{-1}cm^{-1}$], $\lambda$ – wavelength [nm], $c$ – concentration of the solution [M], $l$ – path length [cm].

**Table 1.** The extinction coefficients of ARC-compounds. ARC-1182 and ARC-1063 belong to the ARC-Lum group; [A]: (Vaasa et al. 2009); [B]: (Enkvist et al. 2011); [C]: (Viira 2012)

| Compound | $\varepsilon$ [$M^{-1}$ $cm^{-1}$] | $\lambda$ [nm] |
|---|---|---|
| ARC-1042 | 80000 [A] | 559 |
| ARC-904 | 15000 [A] | 260 |
| ARC-1182 | 250000 [B] | 651 |
| ARC-1063 | 250000 [B] | 654 |
| ARC-1411 | 15000 [C] | 286 |
| ARC-1012 | 15000 [A] | 260 |

## 3.4. Determination of the Active Concentration of PKAc

The active concentration of PKAc was determined before each TGL displacement assay. The direct binding assay based on fluorescence anisotropy was used as described previously (Vaasa et al. 2009). All the assays were performed in a 384-well microplate. The 2-fold dilution series of PKAc, starting from 300 nM, were made in the 5-component buffer and ARC-1042 was added into each well at final concentration of 20 nM. The final volume in each well was 20 µl. The microplate was incubated at 30 °C, with simultaneous shaking at 300 rpm, for 10 minutes and then measured with the microplate reader with fluorescence polarization optical module [excitation at 540 (20) nm, emission at 590 (20) nm]. At each well, three cycles of 200 flashes per cycle was measured. The sensitivity of the detector was adjusted with 20 nM ARC-1042 in a 5-component buffer. The anisotropy and fluorescence intensity values at each point

were obtained and correction factor *k* for the active concentration of the kinase was calculated using the nonlinear regression equation (Equation 6).

$$Y = (1 - M) \times A_f + M \times A_b$$

$$M = \frac{Q \times Z}{[1 + Z \times (Q - 1)]}$$

$$Z = \frac{L_t + K_d + k \times X - \sqrt{(L_t + K_d + k \times X)^2 - 4 \times L_t \times k \times X}}{2 \times L_t}$$

**Equation 6**. The equation of anisotropy, where *Y* is the measured anisotropy, $A_f$ and $A_b$ are the anisotropy values of the free ligand and anisotropy of the ligand in complex, respectively, *Q* is the ratio of the quantum yields of bound and free probe, $L_t$ is the total concentration of the ligand, $K_d$ represents the dissociation constant of the ligand-kinase complex, *X* is the total concentration of the protein kinase, *k* is the ratio of the active (binding) and the reported by the provider concentration of the protein kinase.

### 3.5. Displacement Assays

The displacement assay was used to determine the $K_d$ value of the tested inhibitor by competing with the photoluminescent probe (ARC-Lum). In detail, the dilution series of the tested inhibitor was made with an 8-channel automatic pipette (Appendix 2) and the complex of the ARC-Lum and the kinase was added into very well of the dilution series. Before all of the measurements the microplates were incubated at 30 °C with simultaneous shaking at 300 rpm for 25 minutes and then measured with the microplate reader with fluorescence polarization optical module [excitation at 590 (50) nm, emission at 675 (50) nm] and HTRF optical module [excitation at 337 (50) nm, emission at 675 (50) nm]. The anisotropy, fluorescence and TGL intensities were obtained from each well. The $IC_{50}$ value was determined by the Equation 7, and the $K_d$ was calculated using the Equation 3C. See Figure 6 as an example of a displacement curve.

$$Y = \text{Bottom} + \frac{(\text{Top} - \text{Bottom})}{(1 + 10^{(\text{Log } IC50 - X) * \text{Hill slope})})}$$

**Equation 7.** Nonlinear regression equation for $IC_{50}$ calculation from a displacement curve, where *X* is a logarithm of the inhibitor's concentration; *Y* is a response (e.g. the TGL signal), decreasing as *X* increases; Top and Bottom are the plateau values for the upper and lower plateau in same units as Y; Log$IC_{50}$ is the logarithm of half maximal inhibitory concentration, the same log units as *X*; the Hill slope is the quantified steepness, also called a slope factor.

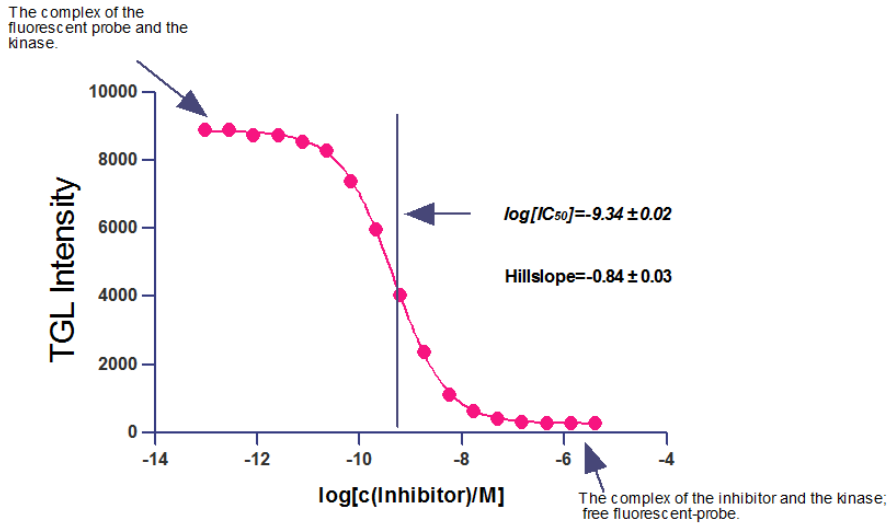


**Figure 6.** An example of a displacement curve**.** The lower plateau is formed in the displacement curve, when the tested inhibitor at higher concentrations is able to completely displace the probe (ARC-Lum) from the complex with a kinase. The ARC-Lum is thus freely in the solution and no TGL signal is produced. The lower the concentration of the competitive inhibitor, the lower is its capability to displace the probe from the complex with a kinase. Finally the higher plateau is formed, where the TGL signal is the highest. The logarithm of the half-maximal inhibitory concentration, which indicates the quantity of the inhibitor needed to displace the probe from 50% of the protein kinase could also be determined from the curve.

## 3.6. Determination of the Suitable BSA Concentration for the Buffer

### 3.6.1. Incubation Time Study

Two displacement curves were made (as described before). Dilution series of ARC-1411 starting from 20 µM were made and the complex of 50 nM ARC-1182 and 1 nM PKAc was added. The first curve was analyzed after 25 minutes of incubation. The second curve was analyzed after 50 minutes of incubation.

### 3.6.2. The Study of the Behavior of ARC-1182 towards BSA

Assay 1. 3-fold dilution series of 50 µM ARC-1411, 100 nM ARC-1182 and 1 nM PKAc in 5-component buffer (7.5 µM BSA) or 4-component buffer were made.

Assay 2. The 2-fold dilution series of BSA was made in the 4-component buffer and ARC-1182 with final concentration of 1 nM or 100 nM was added into each dilution line of the BSA.

Assay 3. 2 replicate points of 100 nM ARC-1182 and ARC-1063 in 4-component buffer and 5-component buffer with 7.5 µM BSA, 50 nM ARC-1182 and ARC-1063 in 5-component buffer with 7.5 µM BSA were made.

All the microplates were incubated at 30 °C with simultaneous shaking at 300 rpm for 25 minutes and then measured with the microplate reader with fluorescence polarization optical module [excitation at 590 (50) nm, emission at 675 (50) nm] and HTRF optical module [excitation at 337 (50) nm, emission at 675 (50) nm] (three cycles of 200 flashes per cycle), respectively. The anisotropy, fluorescence and TGL intensities were measured in each well.

### 3.6.3. The Determination of BSA Concentration for Assays

The 2-fold dilution series of ARC-1182 starting from 400 nM were made in the 4-component buffer and BSA was added at 1.5 µM or 7.5 µM concentration into each dilution line of the ARC-1182. The microplate was measured at the same conditions as in chapter 3.6.2.

## 3.7. Determination of the Optimal Assay Conditions and Affinity

### 3.7.1. Different Conditions for the TGL Method

In order to determine the affinities of ARC-1012, ARC-904 and ARC-1411 and optimal conditions for TGL based displacement measurements, different concentrations of these compounds, PKAc and ARC-1182 were set as different levels of full factorial assays (Table 2, Table 3, Table 4)[2].

**Table 2.** The full factorial design to determine the affinity of ARC-904**.** 27 different levels of TGL-based displacement assays were made and each level was repeated 3 times

| **Compound** | **Concentration level** | | |
|---|---|---|---|
| ARC-904 (µM) | 1 | 4 | 8 |
| PKAc (nM) | 0.1 | 0.5 | 1 |
| ARC-1182 (nM) | 0.1 | 0.5 | 1 |

[2] The concentration level for the inhibitor means the first point of the dilution series.

**Table 3.** The full factorial design to determine the affinity of ARC-1012. 27 different levels of TGL-based displacement assays were made and each level was repeated 3 times

| **Compound** | **Concentration level** | | |
|---|---|---|---|
| ARC-1012 (µM) | 80 | 120 | 180 |
| PKAc (nM) | 0.1 | 0.5 | 1 |
| ARC-1182 (nM) | 0.1 | 0.5 | 1 |

**Table 4.** The full factorial design to determine the affinity of ARC-1411. 36 different levels of TGL-based displacement assays were made and each level was repeated 3 times

| **Compound** | **Concentration level** | | | |
|---|---|---|---|---|
| ARC-1411 (µM) | 5 | 20 | 40 | 80 |
| PKAc (nM) | 0.1 | 0.5 | 1 | |
| ARC-1182 (nM) | 10 | 40 | 80 | |

A 3-fold dilution series of the tested inhibitor (ARC-904, ARC-1012 or ARC-1411) was made into a buffer: in case of ARC-1411, 5-compound buffer with 1.5 µM BSA was used; in case of ARC-904 and ARC-1012, 5-compound buffer with 7.5 µM BSA was used. Finally, the complex of PKAc and ARC-1182, was added into each well. The final volume in each of the wells was 20 µl. All the assays were measured and analyzed as described previously in chapter 3.5.

### 3.7.2. The Parameters to Evaluate the Assay Quality

To determine the optimal assay conditions, different parameters were taken into account for the evaluation (Table 5). The weightage was set intuitively, based on the importance of each parameter. The calculations of score of parameters are based on the Equation 8.

**Table 5.** Parameters for estimating the assay conditions

| **Parameter** | **Weightage** |
|---|---|
| Relative bias of $K_d$ value | 30% |
| Relative standard deviation of $K_d$ value | 15% |
| Z-factor | 15% |
| Relative standard deviation of data points | 15% |
| Outliers | 5% |
| Financial prominence | 20% |

- Score of relative bias of $K_d$ $= [1 - \text{relative bias of } K_d] \times \text{weightage} \times 100$
- Score of $Z - \text{factor} = Z - \text{factor} \times \text{weightage} \times 100$
- Score of relative SD of data points $= (1 - SD_{DP,rel}) \times \text{weightage} \times 100$
- Score of outliers $= (\frac{\text{number of outliers}}{2}) \times \text{weightage} \times 100$
- Score of relative SD of $K_d$ value $= (1 - SD_{Kd,rel}) \times \text{weightage} \times 100$

**Equation 8.** The formulas for score calculations of parameters.

The financial prominence was calculated based on the marketing price and the consumption of the compounds. The final score was calculated by the sum the score of each parameter. The higher the total score, the better is the quality of the assay under the studied conditions.

# 4. Results and Discussion

The importance of the protein kinases as drug targets has caused an increasing need for reliable HTS methods for characterization of new compounds. The best HTS assays require small amount of sample, are time saving and robust, have adequate sensitivity, accuracy, precision and are prone for automation (Zhang et al. 1999). Based on these requirements, the aim of this work was to determine the optimal conditions for previously introduced ARC-Lum based TGL method for determination of affinities of different inhibitors of PKAc by analyzing trueness, precision, screening window coefficient, outliers and economical contribution.

## 4.1. Determination of the Effect of BSA

ARC-1411 is a very high affinity inhibitor towards PKAc. In order to establish the exact affinity of the probe with ARC-Lum based TGL method, high concentration of ARC-1182 (the probe) was required to shift the $IC_{50}$ value (see Equation 3 B) to avoid the tight binding conditions. Tight binding condition refers to the situation where the determined $IC_{50}$ goes down to the half of the concentration of the total kinase present in the solution. The higher the concentration of the probe, the harder it is for the inhibitor to displace the probe from the complex with the protein kinase – this would lead to the higher value of $IC_{50}$.

Unfortunately, several pilot experiments showed that the Hill slope of the curve was below 0.5 and the displacement curve had several inconspicuous plateaus. The figure below (Figure 7) is an example. An interesting phenomenon occurred if the displacement assays at different conditions were compared. The higher the concentration of ARC-1182, the higher the TGL intensity at the lower plateau and the worse the shape of the curve. Such result could be caused by two processes. First, the incubation time might be too short (25 minutes), and the displacement of the probe from the complex is consequently not fully complete. Second, the probe could be simultaneously bound to the kinase and another compound. This interaction could result in lower Hill slope value and the absence of clearly distinguishable lower plateau. If the other compound also has the ability to fix the ARC-Lum in a way that it will emit TGL after excitation, the measurement window could be decreased.

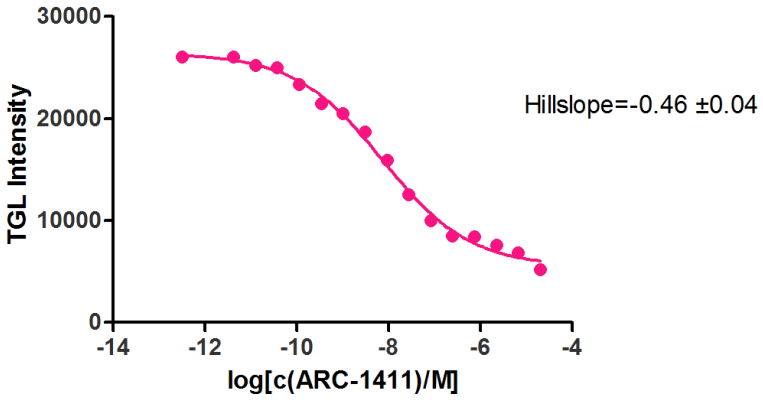


**Figure 7.** Displacement curve of ARC-1411 at 50 nM ARC-1182 and 1 nM PKAc.

### 4.1.1. Incubation Time

As mentioned before, the high intensity level of the lower plateau might be due to the incomplete displacement reaction. Hence, the comparison of the curves incubated during different time spans was made (Figure 8).

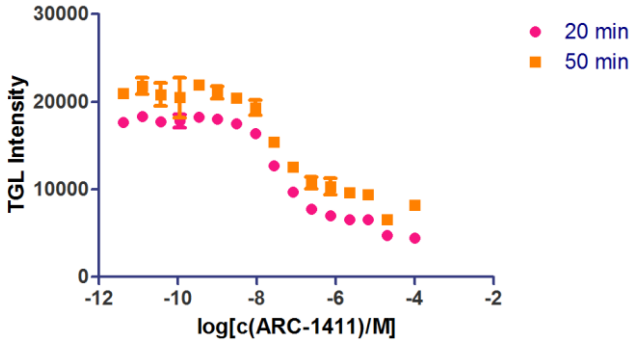


**Figure 8.** The study of different incubation times for a displacement assay, at 50 nM ARC-1182 and 1 nM PKAc.

As it could be seen, the increase of the incubation time did not make distinguishable changes to the shape of the displacement curve, thus it could be stated, that 25 minutes of incubation time is sufficient for ARC-1411 to displace the ARC-1182 from the complex and short incubation time is not the reason that causes the problem described above.

### 4.1.2. Nonspecific Binding of the ARC-Lum Probe

Although normally the TGL signal should be produced only, if an ARC-Lum probe is in complex with the kinase, based on the shape of the previously described curve, there was a suspicion that ARC-Lum might form a complex with other components in the buffer in large excess compared to the kinase. Based on the properties of all substances in the 5-component buffer, BSA as a protein is the most probable compound to associate with ARC-Lum probe

leading to a TGL signal. BSA is used in the buffer to prevent PKAc and the probe from binding to the walls of the microplate wells and to protect PKAc from environmental damages (Xiao & Isaacs 2012).

To study whether the interference came from the complex formed by BSA and ARC-1182, the displacement assays in the presence and absence of BSA were carried out (Figure 9). As it could be seen, although the shape of the curve was improved, the TGL signal of the higher plateau has also decreased by three-fold. Here, the question arises – whether BSA prevents the kinase and the probe from binding to the walls, or does it form complex with the ARC-Lum probe.

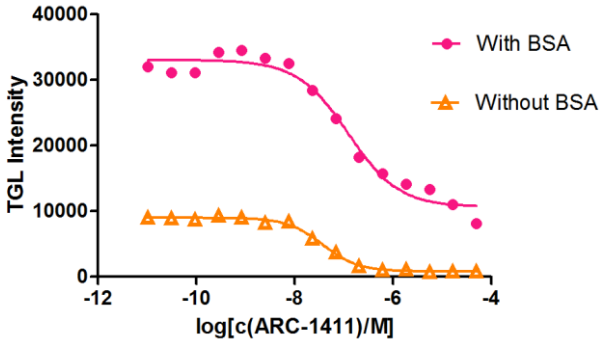


**Figure 9.** Displacement assay with 5-component buffer and with 4-component buffer at 100 nM ARC-1182 and 1 nM PKAc. Concentration of BSA was 7.5 µM.

Based on these questions, several experiments were performed which are described in chapter 3.6.2. Figure 10 A and Figure 10 B show the assay of dilution series of BSA with different concentration of ARC-1182. In Figure 10 A, the higher the concentration of BSA, the higher the TGL signal intensity when log[c(BSA)/M] is over approximately -6. It could be claimed that BSA and ARC-1182 formed a complex which gave the nonspecific TGL signal. When the concentration of BSA is below 1 µM, the effect of the binding is not obvious compared to higher BSA concentrations. In Figure 10 B, the fluorescence intensity was observed and it could be seen that at 100 nM ARC-1182 the fluorescence intensity was constant, indicating that the amount of the ARC-1182 in the solution is also constant. On the other hand, at 1 nM ARC-1182 a significant amount of the probe did not contribute to the fluorescence intensity – indicating its attachment to the walls. These results further prove the necessity of the presence of BSA in the assay buffer as an anti-adsorption agent.

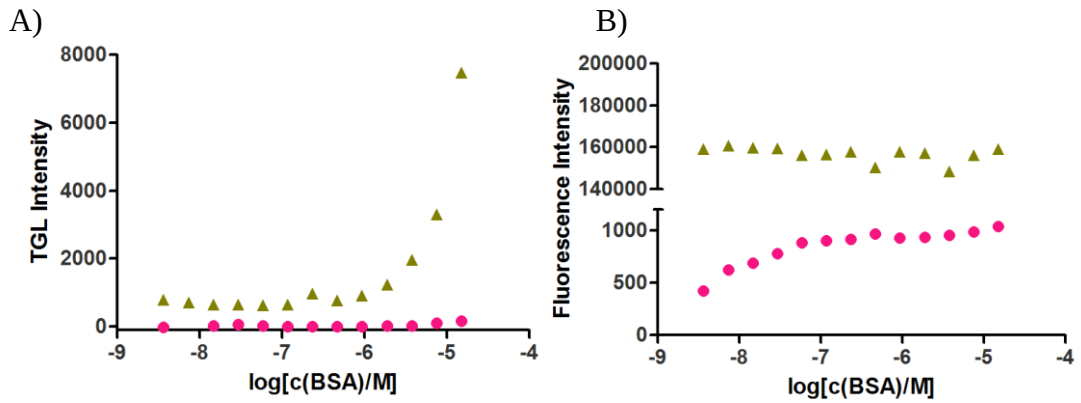


**Figure 10.** A) The TGL intensity of dilution series of BSA with different concentrations of ARC-1182; B) The fluorescence intensity of dilution series of BSA with different concentrations of ARC-1182. In both graphs: green triangles – 100 nM ARC-1182, pink circles – 1 nM ARC-1182.

In order to know at which concentration of ARC-1182 the TGL signal is less influenced by BSA, a dilution series of ARC-1182 at different concentrations of BSA was studied. Figure 11 points to increased effect of BSA at higher than ~3 nM ARC-1182 concentrations. As it can be seen from the results of the study BSA at 1.5 µM concentration increases the signal less than at 7.5 µM concentration.

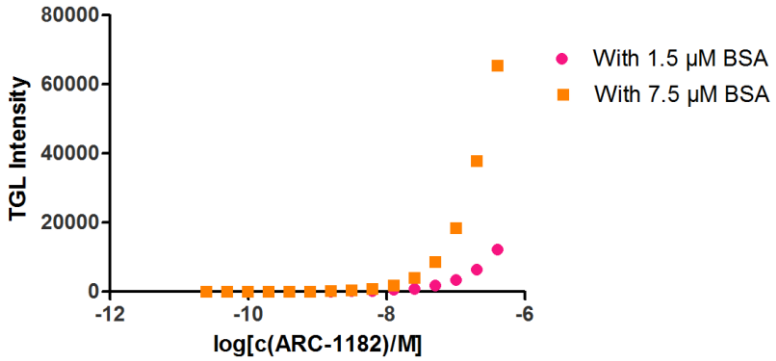


**Figure 11.** Dilution series of ARC-1182 in the presence of 7.5 µM and 1.5 µM BSA.

To establish the cause of the nonspecific association of BSA and ARC-1182, the comparison of behavior of two ARC-Lum probes ARC-1182 and ARC-1063 in assay conditions was carried out. ARC-1063 has almost the same structure as ARC-1182 but has a different dye attached to it. ARC-1063 is labeled with an Alexa Fluor 647 and ARC-1182 with a PromoFluor-647. As these two dyes have similar optical properties, ARC-1182 and ARC-1063 have almost the same luminescence characteristics (Enkvist et al. 2011).

The increase in the concentration of these two probes in the presence of BSA results in increase in the TGL intensity (Figure 12). The study revealed that ARC-1182 is more sensitive to the presence of BSA than ARC-1063. Thus it could be speculated that the association with BSA is

influenced by the structure of the dye. Nevertheless, as Alexa Fluor 647 is more expensive than PromoFluor-647, ARC-1182 was still consider to be a better candidate for HTS assays.

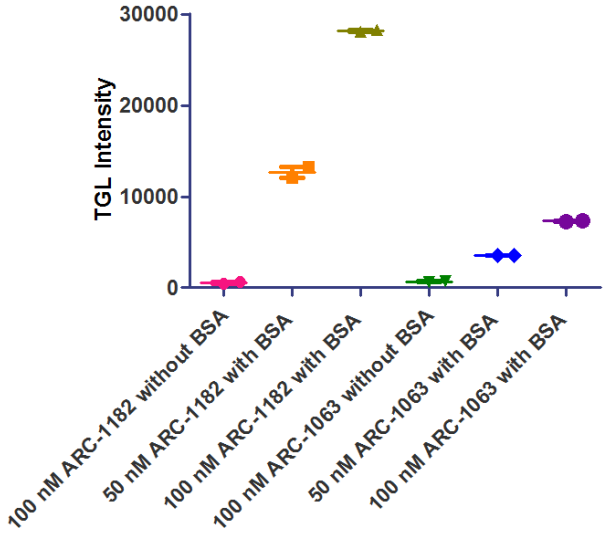


**Figure 12.** The comparison of optical properties of ARC-1182 and ARC-1063 at different concentrations and in different assay buffers.

To sum up the analysis of the influence of BSA, the following conclusions were made. Due to the high concentrations of ARC-1182 used in the analysis of high-affinity inhibitors, 1.5 µM BSA is recommended in order to avoid nonspecific TGL signal. Analysis where lower concentrations of ARC-1182 are used, 7.5 µM BSA is more suitable, as it helps to prevent the adsorption of the probe to the walls of the microplate wells and pipette tips.

## 4.2. Analysis of the Parameters

The ARC-Lum based TGL assay conditions were optimized for the analyses of inhibitors with different affinities towards PKAc. In order to evaluate the quality of the assay,the following parameters were analyzed: the relative bias of $K_d$, relative SD of $K_d$, Z-factor, relative SD of data points, outliers and financial prominence.

### 4.2.1. Analysis of Relative Bias of $K_d$

The relative bias of $K_d$ indicates the trueness of the assay. The influence of different concentrations of PKAc, ARC-1182 and ARC-1012 on $K_d$ was studied. It was found, that the first point of the dilution series has the most significant influence on the bias (Figure 13). The higher the concentration the dilution series is started at, the lower is the bias. When the dilution series is started at lower concentrations, there are only a few points in the lower plateau. If any of them is deviating from the plateau, influence on the shape of the curve is more significant

than in case of greater number of points. The final $K_d$ determined is thus more easily biased. The bias of the $K_d$ is not effected by different concentrations of ARC-1182 and PKAc used.

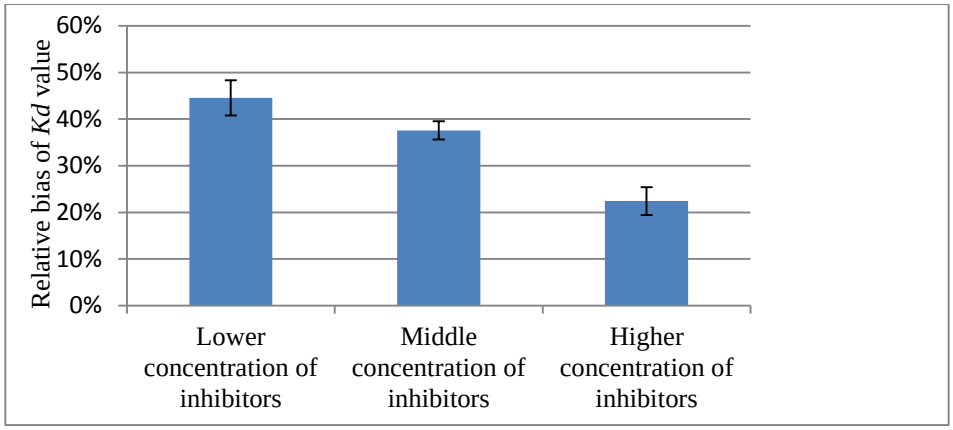


**Figure 13.** The relative bias of $K_d$ values at different concentration level of inhibitors. Lower concentration of inhibitors are the average of relative bias of $K_d$ of 80 µM of ARC-1012, 1 µM of ARC-904 and 5 µM of ARC-1411. Middle concentration of inhibitors are the average of relative bias of $K_d$ of 120 µM of ARC-1012, 4 µM of ARC-904 and mean of 20 µM and 40µM of ARC-1411. Higher concentration of inhibitors are the average of relative bias of $K_d$ of 180 µM of ARC-1012, 8 µM of ARC-904 and 80 µM of ARC-1411.

### 4.2.2. The Analysis of Relative SD of $K_d$

The relative SD of $K_d$ is a parameter, which estimates the repeatability – reflecting how much $K_d$ values determined from parallel curves differ from each other. The influence of different concentrations of PKAc, ARC-1182 and ARC-1012 on the parameter was studied. The obtained results are similar to the previous deduction of the bias. The few deviations at the lower plateau points influence the determination of the affinity and thus SD.

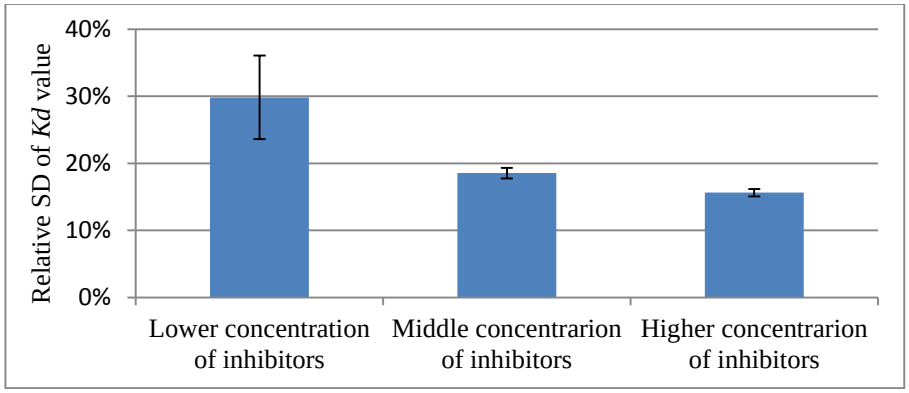


**Figure 14.** The relative SD of $K_d$ values at different concentration level of inhibitors. Lower concentration of inhibitors are the average of relative SD of $K_d$ of 80 µM of ARC-1012, 1 µM of ARC-904 and 5 µM of ARC-1411. Middle concentration of inhibitors are the average of relative SD of $K_d$ of 120 µM of ARC-1012, 4 µM of ARC-904 and 20 µM of ARC-1411. Higher concentration of inhibitors are the average of relative SD of $K_d$ of 180 µM of ARC-1012, 8 µM of ARC-904 and 40µM of ARC-1411.

### 4.2.3. The Analysis of Z-factor

Z-factor is used to evaluate the robustness of the method via analysis of measurement window and the signal to noise ratio: the separation and the variation of upper and lower plateau values of displacement curves. A relationship between the assay window and Z-factor was described in the figure below (Figure 15).

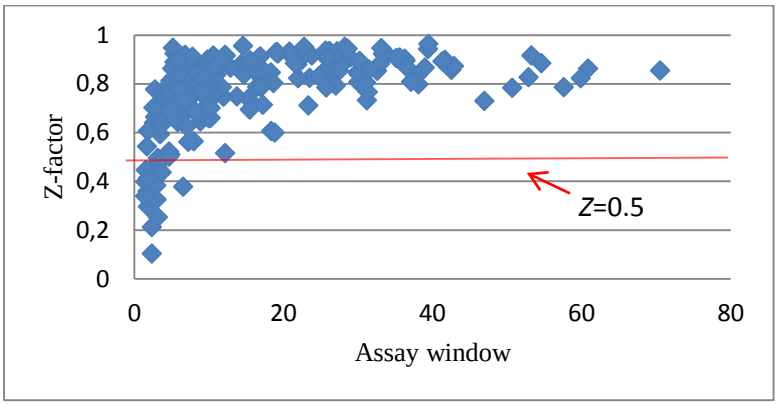


**Figure 15.** The relationship between Z-factor and assay window.

Figure 15 shows that with the increase of the assay window, the Z-factor increases. When the measurement window is over 5, almost all of the determined Z-factors are over 0.5 demonstrating excellent assay conditions. Appendix 3 describes the assay conditions, at which Z-factor is below 0.5 and the data reveals that when the concentration of ARC-1182 is more than 100 times higher than the concentration of PKAc, the Z-factor is quite small. This is due to two reasons. First, the low concentrations of PKAc leads to the low concentration of the complex, thus the TGL signal is low. Secondly, the large amount of ARC-1182 in excess tends to form a complex with BSA, thus resulting in high background signal and higher sensitivity towards errors.

### 4.2.4. The Analysis of Relative SD of Data Points

Relative SD of data points is also used to estimate the repeatability, the difference of this parameter to relative SD of $K_d$ is that this parameter estimates the variation between each data point at same conditions.

The analysis of relative SD of data points revealed that in case of ARC-904 and ARC-1012 (Figure 16) the lower the concentrations of the kinase and the probe, the higher is the relative SD of the data points. This could be caused by the nonspecific binding of the substances to the

walls of the pipette tip or the microplate well. The lower the concentration of the substance the higher proportion of it is adsorbed. There were no significant trends in the SD in case of ARC-1411.

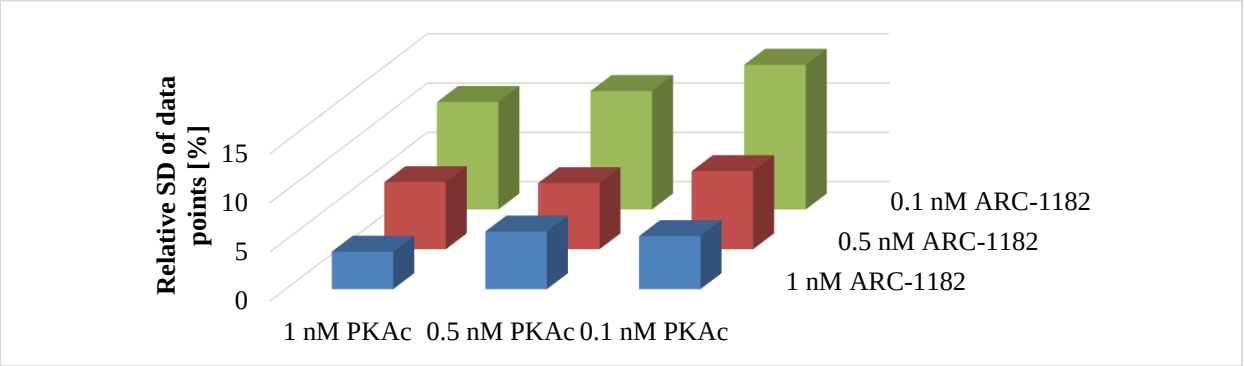


**Figure 16.** The average of relative SD of data points of ARC-904 and ARC-1012 assays in case of different concentrations of PKAc and ARC-1182.

### 4.2.5. The Analysis of Outliers

Outlier analysis expresses the robustness of the assay. This parameter does not only depend on the assay conditions, but also on the operator and devices. Hence, only 5% of weightage was given to the parameter.

The result shows that in case of ARC-1411 (Figure 17), the number of outliers increases if the concentration of PKAc decreases and the concentration of ARC-1182 increases. However, in case of ARC-904 and ARC-1012 (Figure 18), the number of outliers increases when the concentration of the ARC-1182 and PKAc decreases. Interestingly, in ARC-1411 assays the outliers were positioned throughout the displacement curve. In contrast, in the assays of relatively lower affinity inhibitors (ARC-904 and ARC-1012) the outliers were more bunched together to the lower plateau. In case of ARC-1411, there is a large amount of the probe in excess, which is eager to bind to the BSA. The errors in pipetting *e.g.* the buffer (and consequently BSA), are immediately reflected in the TGL signal intensity. The outliers in the lower plateau of the ARC-904 and ARC-1012 displacement curves are mostly likely caused by the low signal to noise ratio.

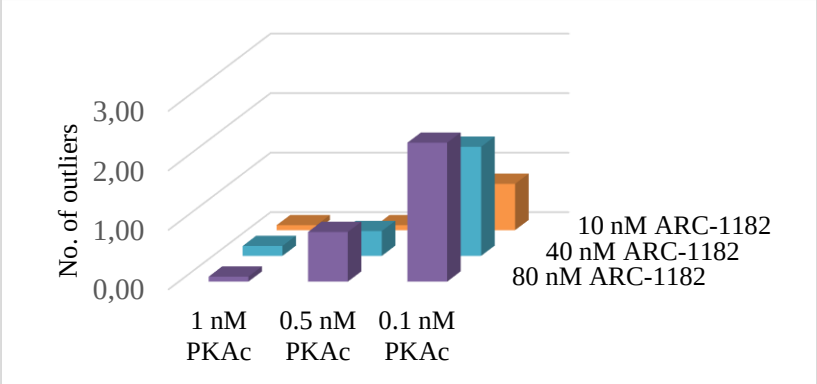


**Figure 17.** The average number of outliers in ARC-1411 assay in case of different concentrations of PKAc and ARC-1182.

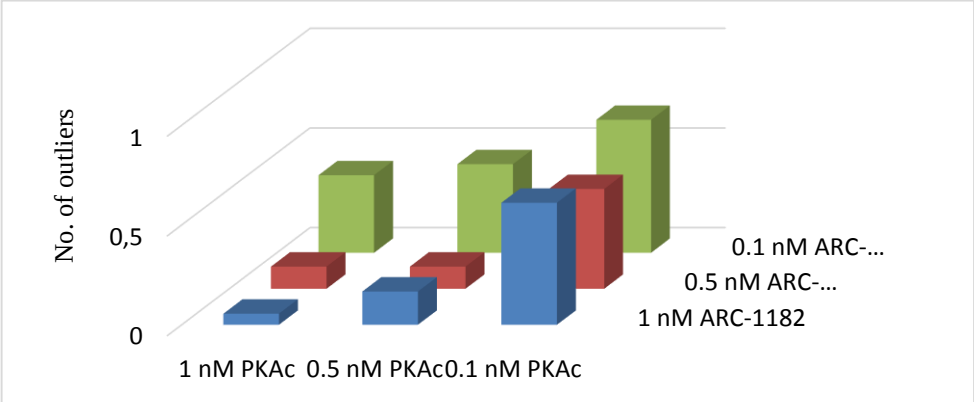


**Figure 18.** The average number of outliers in ARC-904 and ARC-1012 assay in case of different concentrations of PKAc and ARC-1182.

### 4.2.6. Financial Prominence

The financial prominence takes into account the cost of the compounds used in the displacement assays based on the marketing price. Understandably, the higher the amount of substances used in the assay, the more expensive it is. In case of ARC-1411 (Figure 19), the most critical factor influencing the price was the high concentration of ARC-1182 needed. Although high concentrations of the ARC-1411 were also used, the latter did not affect the overall price so much, as the probe ARC-1182 is much more expensive due to the price of the dye attached to it. In case of ARC-1012 (Figure 19), low concentrations of the probe and kinase were used, but as it was not as affine inhibitor as the probe itself, the higher concentrations of it were needed in order to obtain the full displacement curve. Thus the main influence on the price, when the $K_d$ of the inhibitor is more than 10 times higher than the one of the probe, is the amount of inhibitor used. As in case of ARC-904 the $K_d$ is around subnanomolar, the low concentrations of the inhibitor, the kinase and the inhibitor were used.

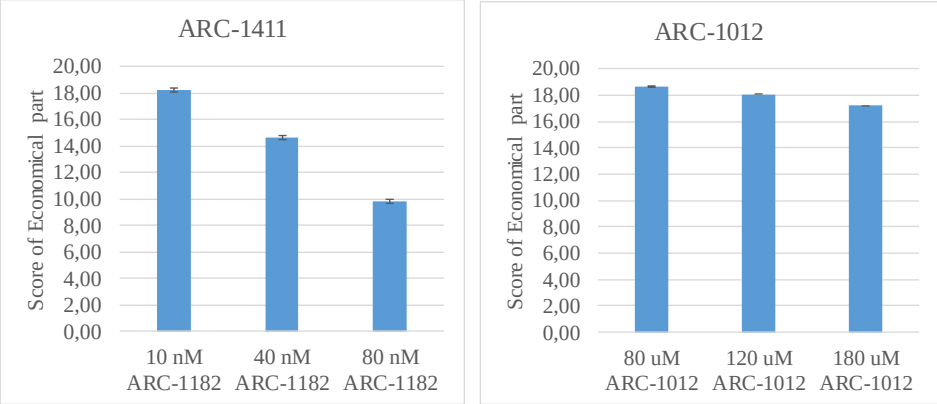


**Figure 19.** The influence on the score of economical estimation of ARC-1182 in ARC-1411 assays and of ARC-1012 in ARC-1012 assays.

## 4.3. The Optimal Conditions for ARC-Lum Based Assay

ARC-1012, ARC-904 and ARC-1411 were chosen to represent the inhibitors which possess low nanomolar, subnanomolar and picomolar affinity towards PKAc, respectively. The optimal conditions were determined based on the analysis of all of the parameters by calculating the total score (Appendixes 4-6). It should be noted, that in case of low picomolar inhibitors, higher concentrations of the probe should be used in order to avoid the tight-binding conditions. In case of nanomolar inhibitors, the dilution series should be started at higher concentrations in order to obtain a complete displacement curve.

**Table 6**. The optimal conditions for tested inhibitors

| | **Reference $K_d$ value (SD)** | **Optimal condition** |
|---|---|---|
| ARC-1012 | 2.5 (0.8) nM | 0.1 nM PKAc; 1nM ARC-1182; 180 µM ARC-1012 |
| ARC-904 | 0.22 (0.04) nM | 0.5 nM PKAc; 0.1 nM ARC-1182; 4 µM ARC-904 |
| ARC-1411 | 0.008 (0.002) nM | 0.5 nM PKAc; 10 nM ARC-1182; 20 µM ARC-1411 |

# Summary

The aim of this master's thesis was the determination of optimal conditions for ARC-Lum based time-gated photoluminescence measurements to determine the affinity of protein kinase inhibitors.

Firstly, the optimal composition of the measurement buffer was established. The analysis revealed that due to the origin of the dye attached to the ARC-1182, the probe binds non-specifically to BSA at higher concentrations. Simultaneously, results of the measurements pointed to the necessity of presence of BSA protein as an anti-adsorption agent in the assay buffer if ARC-1182 probe was applied at lower concentrations. Consequently, adequate concentration of BSA was established to achieve a minimal non-specific TGL signal and minimal adsorption of the probe and protein on walls of the microplate and pipette tips.

Secondly, the relevance of different assay conditions was analysed based on six parameters. The results revealed that too low starting concentration of the inhibitor in the dilution series was the prominent reason to cause the bias of $K_d$ values and high relative SD of $K_d$. The latter phenomenon was most likely caused by the incompleteness of the displacement curve. The Z-factor and the number of outliers were mostly affected by the concentration ratio of ARC-1182 and PKAc. If the probe was used in large excess, the TGL signal was sensitive towards non-specific binding of BSA to the ARC-Lum probe. On the other hand, the lower concentrations of the probe and the kinase caused higher signal to noise ratio. The cost of the assay was mainly prescribed by the affinity of the inhibitors: in case of very high affinity inhibitors, the amount of the probe was the critical factor; in case of low-affinity inhibitors, the amount of the inhibitor was the determining factor.

In this thesis, approximately 8000 analytical data points were processed for optimization of the ARC-Lum based TGL assay. The results obtained can be applied for the development of ARC-Lum probes and for determination of affinity of inhibitors in drug development process. Furthermore, the thesis offers valuable information for further adaption of the assay format to measurements in biological matrixes, for example cell lysates and bodily fluids.

# ARC-Lum sondidel põhinev aeg-lahutatud fotoluminestsentsmeetodi optimeerimine kinaasiinhibiitorite afiinsuse määramiseks

Shanshan Wu

## Kokkuvõte

Käesoleva töö eesmärgiks oli optimeerida aeglahutatud fotoluminestsentsmeetodi tingimusi kinaasiinhibiitorite afiinsuse hindamiseks kolme erineva inhibiitori näite põhjal. Töös analüüsiti ligi 8000 katsepunkti, mille käigus optimeeriti puhvri koostisosad, määrati erinevate inhibiitorite afiinsuse hindamiseks optimaalseimad tingimused ja vaadeldi, kuidas kinaasi, sondi ja inhibiitori kontsentratsioonid mõjutavad erinevaid meetodi kvaliteeti kirjeldavaid parameetreid.

Esmalt optimeeriti puhvri komponentide sisaldus. Katsete tulemusena selgus, et ARC-1182 assotsieerub BSA-ga mittespetsiifiliselt, mille tulemusena emiteerub proovi ergastamisel pika eluealist luminestsentssignaali. Samuti tehti kindlaks, et madalatel sondi kontsentratsioonidel on BSA vajalik, et vältida sondi seostumist mikroplaadile ja pipetiotsikutele. Vastavalt saadud tulemustele kasutati kõrgetel sondi kontsentratsioonidel madalamat BSA kontsentratsiooni ja madalatel sondi kontsentratsioonidel kõrgemat BSA kontsentratsiooni.

Järgmisena võrreldi erinevaid katsetingimusi meetodi kvaliteedi kirjeldavate paremeetrite alusel. Selgus, et kui inhibiitori lahjendusseeriat alustada selle liiga madalalt kontsentratsioonilt, ei moodustu täielikku sidumiskõverat, mis omakorda suurendab mõõteviga ja standardhälvet. Kõrge ARC-1182 ja PKAc kontsentratsioonide suhe mõjutab negatiivselt Z-fakorit ja kõrvalekalduvate punktide arvu. Viimane on arvatavasti põhjustatud aeg-lahutusega luminestsentsmeetodi tundlikkusest mittespetsiifilise seostumise suhtes BSAga, kui sondi kontsentratsioon on üle 100 korra kõrgem kui kinaasi kontsentratsioon. Olukorras, kui kinaasi ja sondi kontsentratsioonid on väga madalad, on signaal-müra suhe madal ja kõrvalekalduvate punktide arv keskmisest suurem.

Töö raames analüüsiti ka katsetingimuste finantsilist osakaalu. Selgus, et madalamate afiinsustega inhibiitorite analüüsimisel oli kõige kulukamaks faktoriks kõrge sondi kontsentratsioon, madalamate afiinsustega inhibiitorite analüüsimisel aga kõrge inhibiitori kontsentratsioon.

Töö tulemusi on võimalik kasutada uute ARC-Lum sondide arendusel ja samuti erinevate inhibiitorite afiinsuste määramiseks. Antud töö käigus omandati väärtuslikku informatsiooni, mille abil on võimalik antud meetodit tulevikus rakendada ka erinevates bioloogilistes maatriksites.

# References


Anand, G. S., Krishnamurthy, S., Bishnoi, T., Kornev, A., Taylor, S. S. and Johnson, D. A. (2010) Cyclic AMP- and (Rp)-cAMPS-induced conformational changes in a complex of the catalytic and regulatory (RI{alpha}) subunits of cyclic AMP-dependent protein kinase. *Molecular & cellular proteomics : MCP,* **9,** 2225-2237.

Arai, Y. and Nagai, T. (2013) Extensive use of FRET in biological imaging. *Microscopy-Jpn,* **62,** 419-428.

Bain, J., McLauchlan, H., Elliott, M. and Cohen, P. (2003) The specificities of protein kinase inhibitors: an update. *The Biochemical journal,* **371,** 199-204.

Bain, J., Plater, L., Elliott, M. et al. (2007) The selectivity of protein kinase inhibitors: a further update. *The Biochemical journal,* **408,** 297-315.

Barf, T. and Kaptein, A. (2012) Irreversible Protein Kinase Inhibitors: Balancing the Benefits and Risks. *Journal of medicinal chemistry,* **55,** 6243-6262.

Bazin, H., Preaudat, M., Trinquet, E. and Mathis, G. (2001) Homogeneous time resolved fluorescence resonance energy transfer using rare earth cryptates as a tool for probing molecular interactions in biology. *Spectrochimica acta. Part A, Molecular and biomolecular spectroscopy,* **57,** 2197-2211.

Bogan, A. A. and Thorn, K. S. (1998) Anatomy of hot spots in protein interfaces. *Journal of molecular biology,* **280,** 1-9.

Bogoyevitch, M. A., Barr, R. K. and Ketterman, A. J. (2005) Peptide inhibitors of protein kinases - discovery, characterisation and use. *Bba-Proteins Proteom,* **1754,** 79-99.

Bogoyevitch, M. A. and Fairlie, D. P. (2007) A new paradigm for protein kinase inhibition: blocking phosphorylation without directly targeting ATP binding. *Drug Discov Today,* **12,** 622-633.

Bridges, A. J. (2001) Chemical inhibitors of protein kinases. *Chemical reviews,* **101,** 2541-2572.

Cheng, Y. and Prusoff, W. H. (1973) Relationship between the inhibition constant (Ki) and the concentration of inhibitor which causes 50 percent inhibition (I50) of an enzymatic reaction. *Biochemical Pharmacology,* **22,** 3099-3108.

Cohen, P. and Alessi, D. R. (2013) Kinase drug discovery--what's next in the field? *ACS chemical biology,* **8,** 96-104.

Cravatt, B. F., Wright, A. T. and Kozarich, J. W. (2008) Activity-based protein profiling: from enzyme chemistry to proteomic chemistry. *Annual review of biochemistry,* **77,** 383-414.

Davies, S. P., Reddy, H., Caivano, M. and Cohen, P. (2000) Specificity and mechanism of action of some commonly used protein kinase inhibitors. *The Biochemical journal,* **351,** 95-105.

Deng, W. Q., Asma, S. and Pare, G. (2014) Meta-analysis of SNPs involved in variance heterogeneity using Levene's test for equal variances. *European journal of human genetics : EJHG,* **22,** 427-430.

Didier, P., Sharma, K. K. and Mély, Y. (2011) Fluorescence Techniques to Characterise Ligand Binding to Proteins. In: *Biophysical Approaches Determining Ligand Binding to Biomolecular Targets* (S. Neidle, A. Podjarny, A. P. Dejaegere and B. Kieffer eds.). Royal Society of Chemistry, Cambridge, UK.

Ehrlich, N., Christensen, A. L. and Stamou, D. (2011) Fluorescence anisotropy based single liposome assay to measure molecule-membrane interactions. *Analytical chemistry,* **83,** 8169-8176.

Enkvist, E., Lavogina, D., Raidaru, G., Vaasa, A., Viil, I., Lust, M., Viht, K. and Uri, A. (2006) Conjugation of adenosine and hexa-(D-arginine) leads to a nanomolar bisubstrate-analog inhibitor of basophilic protein kinases. *Journal of medicinal chemistry,* **49,** 7150-7159.

Enkvist, E., Vaasa, A., Kasari, M., Kriisa, M., Ivan, T., Ligi, K., Raidaru, G. and Uri, A. (2011) Protein-induced long lifetime luminescence of nonmetal probes. *ACS chemical biology,* **6,** 1052-1062.

Enkvist, E., Viht, K., Bischoff, N., Vahter, J., Saaver, S., Raidaru, G., Issinger, O. G., Niefind, K. and Uri, A. (2012) A subnanomolar fluorescent probe for protein kinase CK2 interaction studies. *Organic & biomolecular chemistry,* **10,** 8645-8653.

Fedorov, O., Muller, S. and Knapp, S. (2010) The (un)targeted cancer kinome. *Nature chemical biology,* **6,** 166-169.

Förster, T. (1946) Energiewanderung und Fluoreszenz. Naturwissenschaften **33,** 166-175.

Gribble, F. M., Loussouarn, G., Tucker, S. J., Zhao, C., Nichols, C. G. and Ashcroft, F. M. (2000) A novel method for measurement of submembrane ATP concentration. *The Journal of biological chemistry,* **275,** 30046-30049.

Hanks, S. K. and Hunter, T. (1995) Protein kinases 6. The eukaryotic protein kinase superfamily: kinase (catalytic) domain structure and classification. *FASEB journal :*

*official publication of the Federation of American Societies for Experimental Biology,* **9,** 576-596.

Hanks, S. K., Quinn, A. M. and Hunter, T. (1988) The protein kinase family: conserved features and deduced phylogeny of the catalytic domains. *Science (New York, N.Y.),* **241,** 42-52.

Hines, A. C. and Cole, P. A. (2004) Design, synthesis, and characterization of an ATP-peptide conjugate inhibitor of protein kinase A. *Bioorganic & medicinal chemistry letters,* **14,** 2951-2954.

Hunter, T. (1987) A thousand and one protein kinases. *Cell,* **50,** 823-829.

Hunter, T. (1994) 1001 protein kinases redux--towards 2000. *Seminars in cell biology,* **5,** 367-376.

Kasari, M., Ligi, K., Williams, J. A., Vaasa, A., Enkvist, E., Viht, K., Palsson, L. O. and Uri, A. (2013) Responsive microsecond-lifetime photoluminescent probes for analysis of protein kinases and their inhibitors. *Biochimica et biophysica acta,* **1834,** 1330-1335.

Kasari, M., Padrik, P., Vaasa, A., Saar, K., Leppik, K., Soplepmann, J. and Uri, A. (2012) Time-gated luminescence assay using nonmetal probes for determination of protein kinase activity-based disease markers. *Analytical biochemistry,* **422,** 79-88.

Kayser-Bricker, K. J., Glenn, M. P., Lee, S. H., Sebti, S. M., Cheng, J. Q. and Hamilton, A. D. (2009) Non-peptidic substrate-mimetic inhibitors of Akt as potential anti-cancer agents. *Bioorganic & medicinal chemistry,* **17,** 1764-1771.

Kayser, K. J., Glenn, M. P., Sebti, S. M., Cheng, J. Q. and Hamilton, A. D. (2007) Modifications of the GSK3beta substrate sequence to produce substrate-mimetic inhibitors of Akt as potential anti-cancer therapeutics. *Bioorganic & medicinal chemistry letters,* **17,** 2068-2073.

Kim, C., Xuong, N. H. and Taylor, S. S. (2005) Crystal structure of a complex between the catalytic and regulatory (RIalpha) subunits of PKA. *Science (New York, N.Y.),* **307,** 690-696.

Kondapalli, L., Soltani, K. and Lacouture, M. E. (2005) The promise of molecular targeted therapies: protein kinase inhibitors in the treatment of cutaneous malignancies. *Journal of the American Academy of Dermatology,* **53,** 291-302.

Krebs, E. G. and Beavo, J. A. (1979) Phosphorylation-dephosphorylation of enzymes. *Annual review of biochemistry,* **48,** 923-959.

Kuznetsov, A., Uri, A., Raidaru, G. and Jarv, J. (2004) Kinetic analysis of inhibition of cAMP-dependent protein kinase catalytic subunit by the peptide-nucleoside conjugate AdcAhxArg6. *Bioorganic chemistry,* **32,** 527-535.

Lakowicz, J. R. (2006): Principle of Fluorescence Spectroscopy. Springer, Baltimore, Maryland, USA.

Lavogina, D., Enkvist, E. and Uri, A. (2010) Bisubstrate inhibitors of protein kinases: from principle to practical applications. *ChemMedChem,* **5,** 23-34.

Lavogina, D., Lust, M., Viil, I., Konig, N., Raidaru, G., Rogozina, J., Enkvist, E., Uri, A. and Bossemeyer, D. (2009) Structural analysis of ARC-type inhibitor (ARC-1034) binding to protein kinase A catalytic subunit and rational design of bisubstrate analogue inhibitors of basophilic protein kinases. *Journal of medicinal chemistry,* **52,** 308-321.

Lawrence, D. S. and Niu, J. (1998) Protein kinase inhibitors: the tyrosine-specific protein kinases. *Pharmacology & therapeutics,* **77,** 81-114.

Lebakken, C. S., Riddle, S. M., Singh, U., Frazee, W. J., Eliason, H. C., Gao, Y., Reichling, L. J., Marks, B. D. and Vogel, K. W. (2009) Development and Applications of a Broad-Coverage, TR-FRET-Based Kinase Binding Assay Platform. *J Biomol Screen,* **14,** 924-935.

Li, Y., Xie, W. and Fang, G. (2008) Fluorescence detection techniques for protein kinase assay. *Analytical and bioanalytical chemistry,* **390,** 2049-2057.

Lindsley, C. W., Barnett, S. F., Yaroschak, M., Bilodeau, M. T. and Layton, M. E. (2007) Recent progress in the development of ATP-competitive and allosteric Akt kinase inhibitors. *Current topics in medicinal chemistry,* **7,** 1349-1363.

London, N., Movshovitz-Attias, D. and Schueler-Furman, O. (2010) The structural basis of peptide-protein binding strategies. *Structure (London, England : 1993),* **18,** 188-199.

Loog, M., Uri, A., Raidaru, G., Jarv, J. and Ek, P. (1999) Adenosine-5 '-carboxylic acid peptidyl derivatives as inhibitors of protein kinases. *Bioorganic & medicinal chemistry letters,* **9,** 1447-1452.

Manning, G., Whyte, D. B., Martinez, R., Hunter, T. and Sudarsanam, S. (2002) The protein kinase complement of the human genome. *Science (New York, N.Y.),* **298,** 1912-1934.

Masterson, L. R., Mascioni, A., Traaseth, N. J., Taylor, S. S. and Veglia, G. (2008) Allosteric cooperativity in protein kinase A. *Proceedings of the National Academy of Sciences of the United States of America,* **105,** 506-511.

Mathis, G. (1993) Rare earth cryptates and homogeneous fluoroimmunoassays with human sera. *Clinical chemistry,* **39,** 1953-1959.

Mathis, G. (1995) Probing Molecular-Interactions with Homogeneous Techniques Based on Rare-Earth Cryptates And Fluorescence Energy-Transfer. *Clinical chemistry,* **41,** 1391-1397.

Nikolovska-Coleska, Z., Wang, R., Fang, X. et al. (2004) Development and optimization of a binding assay for the XIAP BIR3 domain using fluorescence polarization. *Analytical biochemistry,* **332,** 261-273.

Parang, K. and Cole, P. A. (2002) Designing bisubstrate analog inhibitors for protein kinases. *Pharmacology & therapeutics,* **93,** 145-157.

Parang, K., Till, J. H., Ablooglu, A. J., Kohanski, R. A., Hubbard, S. R. and Cole, P. A. (2001) Mechanism-based design of a protein kinase inhibitor. *Nature structural biology,* **8,** 37-41.

Reischl, U., Bretagne, S., Kruger, D., Ernault, P. and Costa, J. M. (2003) Comparison of two DNA targets for the diagnosis of Toxoplasmosis by real-time PCR using fluorescence resonance energy transfer hybridization probes. *BMC infectious diseases,* **3,** 7.

Ricouart, A., Gesquiere, J. C., Tartar, A. and Sergheraert, C. (1991) Design of potent protein kinase inhibitors using the bisubstrate approach. *Journal of medicinal chemistry,* **34,** 73-78.

Riddle, S. M., Vedvik, K. L., Hanson, G. T. and Vogel, K. W. (2006) Time-resolved fluorescence resonance energy transfer kinase assays using physiological protein substrates: applications of terbium-fluorescein and terbium-green fluorescent protein fluorescence resonance energy transfer pairs. *Analytical biochemistry,* **356,** 108-116.

Schneider, T. L., Mathew, R. S., Rice, K. P., Tamaki, K., Wood, J. L. and Schepartz, A. (2005) Increasing the kinase specificity of k252a by protein surface recognition. *Organic letters,* **7,** 1695-1698.

Schwartz, P. A. and Murray, B. W. (2011) Protein kinase biochemistry and drug discovery. *Bioorganic chemistry,* **39,** 192-210.

Shapiro, S. S. and Wilk, B. M. (1965) An Analysis of Variance Test for Normality (Complete Samples). *Biometrika,* **52,** 591-611.

Sjoberg, T. J., Kornev, A. P. and Taylor, S. S. (2010) Dissecting the cAMP-inducible allosteric switch in protein kinase A RIalpha. *Protein science : a publication of the Protein Society,* **19,** 1213-1221.

Sourjik, V. and Berg, H. C. (2002) Binding of the Escherichia coli response regulator CheY to its target measured in vivo by fluorescence resonance energy transfer. *Proceedings of the National Academy of Sciences of the United States of America*, **99,** 12669-12674.

Uri, A., Lust, M., Vaasa, A., Lavogina, D., Viht, K. and Enkvist, E. (2010) Bisubstrate fluorescent probes and biosensors in binding assays for HTS of protein kinase inhibitors. *Biochimica et biophysica acta,* **1804,** 541-546.

Vaasa, A., Ligi, K., Mohandessi, S., Enkvist, E., Uri, A. and Miller, L. W. (2012) Time-gated luminescence microscopy with responsive nonmetal probes for mapping activity of protein kinases in living cells. *Chemical communications (Cambridge, England),* **48,** 8595-8597.

Vaasa, A., Lust, M., Terrin, A., Uri, A. and Zaccolo, M. (2010) Small-molecule FRET probes for protein kinase activity monitoring in living cells. *Biochemical and biophysical research communications,* **397,** 750-755.

Vaasa, A., Viil, I., Enkvist, E., Viht, K., Raidaru, G., Lavogina, D. and Uri, A. (2009) High-affinity bisubstrate probe for fluorescence anisotropy binding/displacement assays with protein kinases PKA and ROCK. *Analytical biochemistry,* **385,** 85-93.

Viht, K., Vaasa, A., Raidaru, G., Enkvist, E. and Uri, A. (2005) Fluorometric TLC assay for evaluation of protein kinase inhibitors. *Analytical biochemistry,* **340,** 165-170.

Viira, B. (2012) Synthesis of Inhibitors for Protein Kinases PKA and PKB. Master thesis. University of Tartu, Tartu, Estonia.

Walsh, D. A., Perkins, J. P. and Krebs, E. G. (1968) An adenosine 3',5'-monophosphate-dependant protein kinase from rabbit skeletal muscle. *The Journal of biological chemistry,* **243,** 3763-3765.

Xiao, Y. and Isaacs, S. N. (2012) Enzyme-linked immunosorbent assay (ELISA) and blocking with bovine serum albumin (BSA)--not all BSAs are alike. *Journal of immunological methods,* **384,** 148-151.

Zhang, J. H., Chung, T. D. Y. and Oldenburg, K. R. (1999) A simple statistical parameter for use in evaluation and validation of high throughput screening assays. *J Biomol Screen,* **4,** 67-73.

Zhao, Y. and Tang, Y. (2007) Research progress in protein-protein interactions and their inhibitiors. *Chinese Bulletion of Life Sciences,* **19,** 6.

# Acknowledgements

I would like to first thank to University of Tartu and the group of Asko Uri for giving me the opportunity to study and work for my master thesis. I would also like to express my sincere gratitude to Hedi Sinijärv, who has supervised and very patiently to support my study. I am very grateful to Kadri Ligi, who helped me understand the working of PHERAstar microplate reader and general theory related to my thesis.

I would like to thank all the other group members, Taavi Ivan, Kaido Viht, Darja Lavõgina, Ganesh Babu Manoharan, Erki Enkvist and Marie Kriisa, for the advice related to my thesis.

I also would like to thank to the financial support from European Social Fund's Doctoral Studies and Internationalisation Programme DoRa.

Last but not least, I would like to thank my friends and family, especially my mom for the support and giving encourage to me.

# Appendixes

## **Appendix 1.** Structures of ARCs used in this work

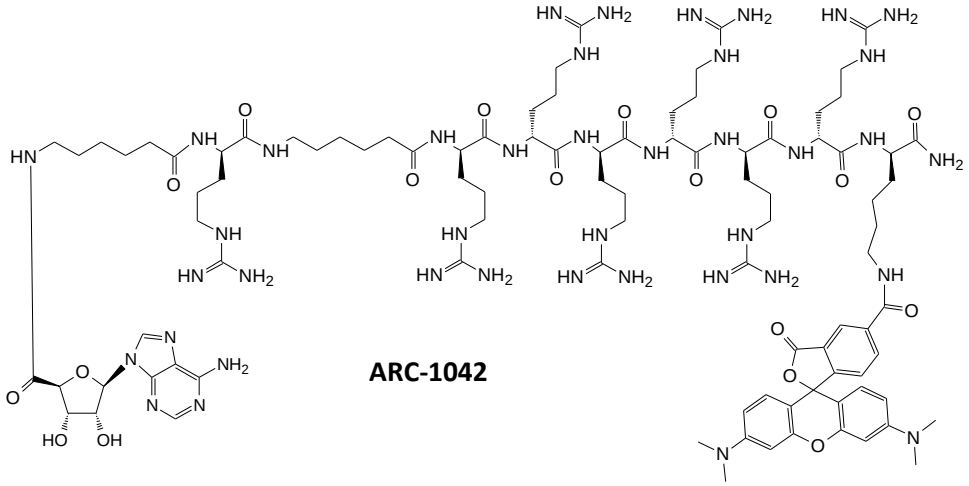

**ARC-1042**

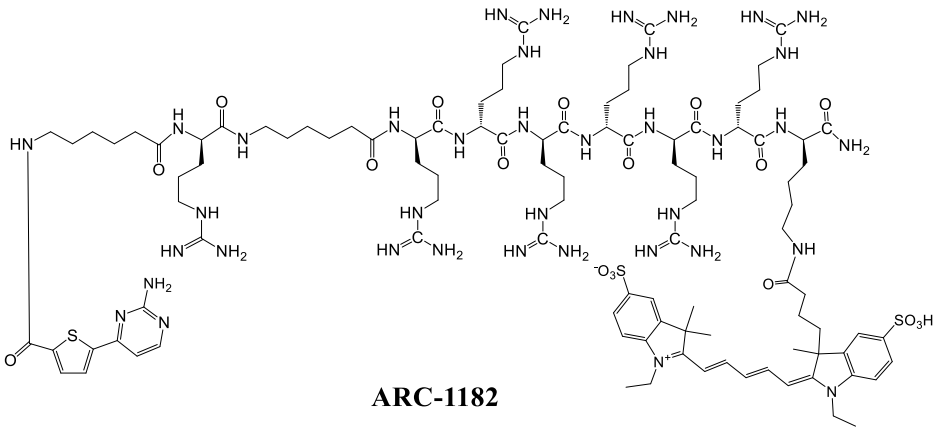

**ARC-1182**

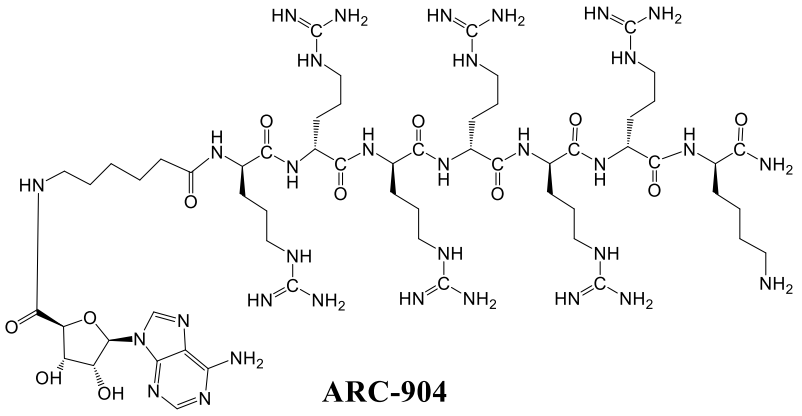

**ARC-904**

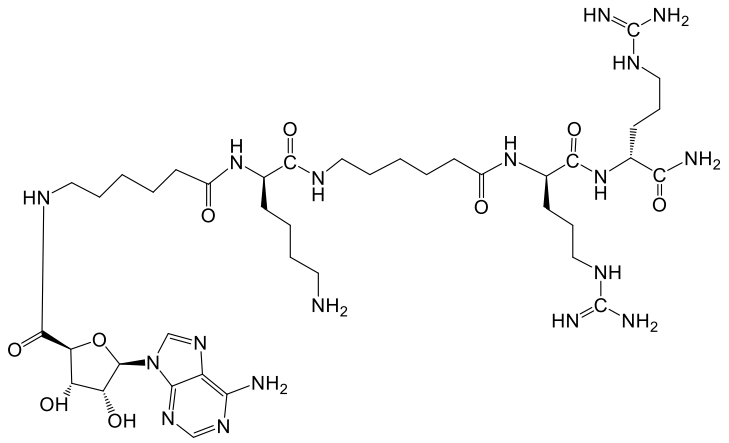

**ARC-1012**

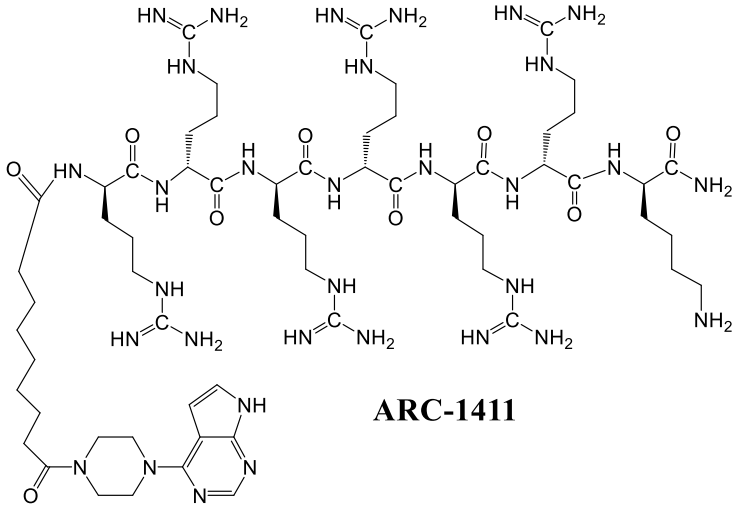

**ARC-1411**

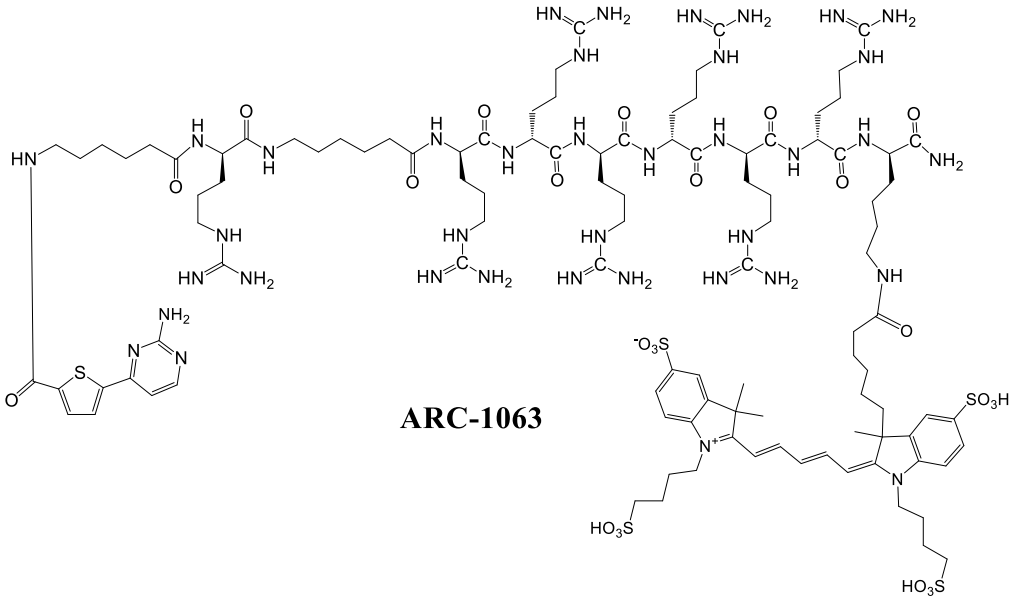

**ARC-1063**

## **Appendix 2.** The 8-channel Automatic Pipette Analysis

20 µl of 1 µM Bodipy FL was pipetted in the well of a microplate by using multi-dispensing mode with 3 replicate measurements (Figure A1). The microplate was incubated at 30 ºC with simultaneous shaking at 300 rpm, for 10 minutes and then measured with the microplate reader with fluorescence intensity optical module [excitation at 485 (12) nm, emission at 520 (15) nm]. The normality (Table A1) was analyzed and homogeneity test (Table A2) of channels based on the data obtained was done.

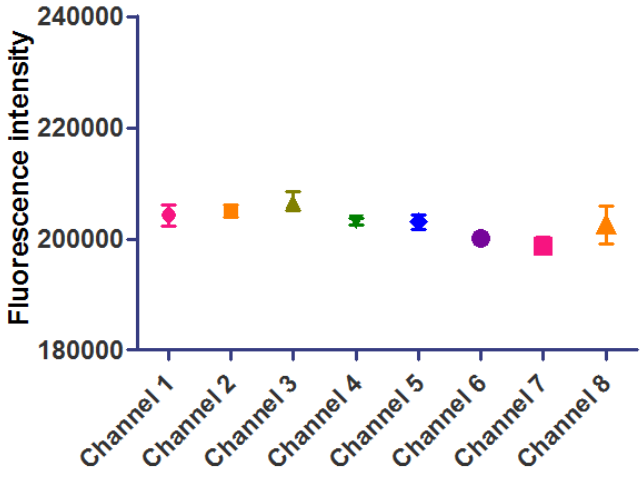


**Figure A 1.** The fluorescence intensity assay for multi-dispensing mode.

**Table A 1.** Test of normality of all of the intensity points

| Shapiro-Wilk | | |
|---|---|---|
| **Statistic** | **Degree of freedom** | **Probability** |
| 0.963 | 24 | 0.512 |

**Table A 2.** Test of homogeneity of variances of intensity points of channels

| Levene Statistic | Degree of freedom 1 | Degree of freedom 2 | Probability |
|---|---|---|---|
| 2.105 | 7 | 16 | 0.103 |

The Shapiro-Wik's test (Shapiro & Wilk 1965) (p=0.512) showed that the data from each channel are approximately normally distributed. Therefore, the parametric Levene's test (Deng *et al.* 2014) was applied which verified the quality of variances in the sample (homogeneity of variance) and the test showed that the probability is 0.103, which is bigger than 0.05, meaning there is no significant difference between channels.

## **Appendix 3.** The Assay Conditions Where the Z-factor was Below 0.5

| **Condition** | **Z-factor** | **Assay window** |
|---|---|---|
| 0.1 nM PKAc; 80nM ARC-1182; 80 µM ARC-1411 | 0.103 | 2.362 |
| 0.1 nM PKAc; 80nM ARC-1182; 80 µM ARC-1411 | 0.123 | 2.360 |
| 0.1 nM PKAc; 10 nM ARC-1182; 5 µM ARC-1411 | 0.253 | 3.153 |
| 0.1 nM PKAc; 80nM ARC-1182; 20 µM ARC-1411 | 0.297 | 1.862 |
| 0.1 nM PKAc; 40 nM ARC-1182; 80 µM ARC-1411 | 0.326 | 3.014 |
| 0.1 nM PKAc; 80nM ARC-1182; 5 µM ARC-1411 | 0.341 | 1.474 |
| 0.1 nM PKAc; 80nM ARC-1182; 20 µM ARC-1411 | 0.360 | 1.817 |
| 1nM PKAc; 0.1 nM ARC-1182; 1 µM ARC-904 | 0.379 | 6.568 |
| 0.1 nM PKAc; 40 nM ARC-1182; 80 µM ARC-1411 | 0.383 | 2.939 |
| 0.1 nM PKAc; 40 nM ARC-1182; 20 µM ARC-1411 | 0.393 | 2.168 |
| 0.1 nM PKAc; 80nM ARC-1182; 5 µM ARC-1411 | 0.398 | 1.505 |
| 0.1 nM PKAc; 80nM ARC-1182; 80 µM ARC-1411 | 0.403 | 2.525 |
| 0.1 nM PKAc; 40 nM ARC-1182; 5 µM ARC-1411 | 0.412 | 1.837 |
| 0.1 nM PKAc; 80nM ARC-1182; 20 µM ARC-1411 | 0.415 | 1.955 |
| 0.1 nM PKAc; 40 nM ARC-1182; 20 µM ARC-1411 | 0.416 | 1.985 |
| 0.1 nM PKAc; 1nM ARC-1182; 1 µM ARC-904 | 0.438 | 3.670 |
| 0.1 nM PKAc; 40 nM ARC-1182; 20 µM ARC-1411 | 0.446 | 2.129 |
| 0.1 nM PKAc; 80nM ARC-1182; 5 µM ARC-1411 | 0.447 | 1.524 |
| 0.1 nM PKAc; 40 nM ARC-1182; 80 µM ARC-1411 | 0.458 | 3.100 |
| 0.1 nM PKAc; 1nM ARC-1182; 1 µM ARC-904 | 0.495 | 3.948 |
| 0.5 nM PKAc; 80 nM ARC-1182; 40 µM ARC-1411 | 0.496 | 3.178 |

**Appendix 4.** The Determination of Optimal Conditions for Measurements with ARC-1012

| Assay conditions | $K_d$ ($SD_{mean}$); (nM) | Weight score of relative bias | Z-factor | Weight score | Relative SD of data points(%) | Weight score | Outlier | Weight score | Relative SD of $K_d$ (%) | Weight score | Economic Weight score | Total score |
|---|---|---|---|---|---|---|---|---|---|---|---|---|
| 1nM PKAc; 1 nM ARC-1182; 80 µM ARC-1012 | 3.1 (0.3) | 22.91 | 0.90 | 13.46 | 3.9 | 14.41 | 0 | 5.00 | 17.7 | 12.35 | 18.55 | 86.68 |
| 1nM PKAc; 0.5 nM ARC-1182; 80 µM ARC-1012 | 3.6 (0.6) | 16.43 | 0.89 | 13.30 | 9.7 | 13.54 | 1 | 4.50 | 30.6 | 10.14 | 18.63 | 76.8 |
| 1nM PKAc; 0.1 nM ARC-1182; 80 µM ARC-1012 | 0.9(0.4) | 11.34 | 0.88 | 13.13 | 27.4 | 10.89 | 3 | 3.50 | 69.4 | 4.58 | 18.69 | 62.13 |
| 0.5 nM PKAc; 1nM ARC-1182; 80 µM ARC-1012 | 2.8 (0.8) | 26.08 | 0.85 | 12.79 | 7.4 | 13.89 | 1 | 4.50 | 47.6 | 7.86 | 18.60 | 83.73 |
| 0.5 nM PKAc; 0.5 nM ARC-1182; 80 µM ARC-1012 | 2.0 (1.1) | 24.31 | 0.86 | 12.89 | 16.9 | 12.46 | 0 | 5.00 | 97.3 | 0.40 | 18.68 | 73.74 |
| 0.5 nM PKAc; 0.1 nM ARC-1182; 80 µM ARC-1012 | 2.9 (0.1) | 25.45 | 0.87 | 13.11 | 16.2 | 12.58 | 1 | 4.50 | 7.9 | 13.82 | 18.74 | 88.19 |
| 0.1 nM PKAc; 1nM ARC-1182; 80 µM ARC-1012 | 2.3 (0.7) | 27.58 | 0.74 | 11.10 | 8.9 | 13.66 | 4 | 3.00 | 56.4 | 6.55 | 18.64 | 80.52 |
| 0.1 nM PKAc; 0.5 nM ARC-1182; 80 µM ARC-1012 | 5.4 (1.1) | -5.4 | 0.82 | 12.37 | 11.3 | 13.31 | 5 | 2.50 | 35.9 | 9.62 | 18.72 | 51.11 |
| | | | | | | | | | | | | |

| | | | | | | | | | | | | |
|---|---|---|---|---|---|---|---|---|---|---|---|---|
| 1nM PKAc; 1 nM ARC-1182; 120 µM ARC-1012 | 1.9 (0.2) | 23.14 | 0.86 | 12.93 | 3.4 | 14.49 | 0 | 5.0 | 15.3 | 12.71 | 17.95 | 86.22 |
| 1nM PKAc; 0.5 nM ARC-1182; 120 µM ARC-1012 | 1.4 (0.4) | 17.31 | 0.84 | 12.66 | 9.8 | 13.53 | 0 | 5.0 | 42.5 | 8.62 | 18.03 | 75.15 |
| 1nM PKAc; 0.1 nM ARC-1182; 120 µM ARC-1012 | 0.9 (0.1) | 10.59 | 0.86 | 12.93 | 10.5 | 13.42 | 1 | 4.5 | 28.1 | 10.79 | 18.09 | 70.32 |
| 0.5 nM PKAc; 1nM ARC-1182; 120 µM ARC-1012 | 1.6 (0.1) | 19.19 | 0.90 | 13.49 | 5.7 | 14.15 | 0 | 5.0 | 13.6 | 12.97 | 18.00 | 82.79 |
| 0.5 nM PKAc; 0.5 nM ARC-1182; 120 µM ARC-1012 | 2.1 (0.3) | 25.72 | 0.87 | 13.07 | 5.8 | 14.13 | 0 | 5.0 | 26.9 | 10.97 | 18.08 | 86.96 |
| 0.5 nM PKAc; 0.1 nM ARC-1182; 120 µM ARC-1012 | 0.8 (0.1) | 9.22 | 0.85 | 12.82 | 22.5 | 11.62 | 3 | 3.5 | 25.7 | 11.15 | 18.14 | 66.44 |
| 0.1 nM PKAc; 1nM ARC-1182; 120 µM ARC-1012 | 3.1 (0.3) | 22.85 | 0.86 | 12.87 | 3.5 | 14.47 | 3 | 3.5 | 19.2 | 12.12 | 18.04 | 83.85 |
| 0.1 nM PKAc; 0.5 nM ARC-1182; 120 µM ARC-1012 | 2.3 (0.1) | 27.74 | 0.78 | 11.77 | 6.4 | 14.03 | 1 | 4.5 | 3.9 | 14.42 | 18.12 | 90.57 |
| 0.1 nM PKAc; 0.1 nM ARC-1182; 120 µM ARC-1012 | 3.1 (0.1) | 23.24 | 0.86 | 12.93 | 12.1 | 13.18 | 2 | 4.0 | 5.4 | 14.19 | 18.18 | 85.71 |
| 1nM PKAc; 1 nM ARC-1182; 180 µM ARC-1012 | 3.2 (0.4) | 21.07 | 0.89 | 13.41 | 5.0 | 14.24 | 0 | 5.0 | 20.2 | 11.96 | 17.05 | 82.74 |

| | | | | | | | | | | | | |
|---|---|---|---|---|---|---|---|---|---|---|---|---|
| 1nM PKAc; 0.5 nM ARC-1182; 180 µM ARC-1012 | 2.8 (0.1) | 26.52 | 0.92 | 13.76 | 4.3 | 14.36 | 1 | 4.5 | 9.1 | 13.64 | 17.13 | 89.90 |
| 1nM PKAc; 0.1 nM ARC-1182; 180 µM ARC-1012 | 1.7 (0.1) | 20.51 | 0.85 | 12.73 | 13.3 | 13.01 | 2 | 4.0 | 8.9 | 13.66 | 17.19 | 81.09 |
| 0.5 nM PKAc; 1nM ARC-1182; 180 µM ARC-1012 | 2.5 (0.1) | 29.35 | 0.82 | 12.27 | 9.4 | 13.58 | 0 | 5.0 | 5.7 | 14.14 | 17.10 | 91.44 |
| 0.5 nM PKAc; 0.5 nM ARC-1182; 180 µM ARC-1012 | 2.5 (0.2) | 29.78 | 0.86 | 12.92 | 6.0 | 14.11 | 2 | 4.0 | 13.7 | 12.95 | 17.18 | 90.93 |
| 0.5 nM PKAc; 0.1 nM ARC-1182; 180 µM ARC-1012 | 1.9 (0.2) | 22.24 | 0.94 | 14.06 | 18.0 | 12.30 | 0 | 5.0 | 22.4 | 11.64 | 17.24 | 82.47 |
| 0.1 nM PKAc; 1nM ARC-1182; 180 µM ARC-1012 | 2.4 (0.1) | 29.18 | 0.82 | 12.27 | 4.5 | 14.32 | 1 | 4.5 | 3.7 | 14.44 | 17.14 | 91.85 |
| 0.1 nM PKAc; 0.5 nM ARC-1182; 180 µM ARC-1012 | 2.4 (0.4) | 28.32 | 0.77 | 11.55 | 10.6 | 13.41 | 0 | 5.0 | 32.2 | 10.17 | 17.22 | 85.67 |
| 0.1 nM PKAc; 0.1 nM ARC-1182; 180 µM ARC-1012 | 1.2 (0.1) | 13.99 | 0.85 | 12.73 | 19.6 | 12.07 | 1 | 4.5 | 13.2 | 13.02 | 17.28 | 73.58 |

## **Appendix 5.** The Estimation of Optimal Conditions for ARC-904

| **Assay conditions** | **$K_d$ ($SD_{mean}$); (nM)** | **Weight score of relative bias** | **Z-factor** | **Weight score** | **Relative SD of data points(%)** | **Weight score** | **Outlier** | **Weight score** | **Relative SD of $K_d$ (%)** | **Weight score** | **Economic Weight score** | **Total score** |
|---|---|---|---|---|---|---|---|---|---|---|---|---|
| 1nM PKAc; 1 nM ARC-1182; 1 μM ARC-904 | 0.218 (0.013) | 29.97 | 0.74 | 11.06 | 4.5 | 14.32 | 1 | 4.50 | 10 | 13.44 | 14.70 | 87.99 |
| 1nM PKAc; 0.5 nM ARC-1182; 1 μM ARC-904 | 0.169 (0.009) | 23.27 | 0.67 | 10.05 | 6.0 | 14.10 | 0 | 5.00 | 19 | 12.19 | 16.20 | 80.81 |
| 1nM PKAc; 0.1 nM ARC-1182; 1 μM ARC-904 | 0.148 (0.017) | 20.46 | 0.52 | 7.80 | 5.8 | 14.12 | 1 | 4.50 | 29 | 10.64 | 17.40 | 74.92 |
| 0.5 nM PKAc; 1nM ARC-1182; 1 μM ARC-904 | 0.100 (0.011) | 13.87 | 0.80 | 11.94 | 5.1 | 14.23 | 0 | 5.00 | 8.7 | 13.69 | 15.70 | 74.43 |
| 0.5 nM PKAc; 0.5 nM ARC-1182; 1 μM ARC-904 | 0.164 (0.020) | 22.60 | 0.72 | 10.80 | 5.0 | 14.24 | 0 | 5.00 | 21 | 11.83 | 17.20 | 81.67 |
| 0.5 nM PKAc; 0.1 nM ARC-1182; 1 μM ARC-904 | 0.1280 (0.003) | 17.64 | 0.56 | 8.45 | 4.9 | 14.26 | 2 | 4.00 | 20 | 11.96 | 18.40 | 74.70 |
| 0.1 nM PKAc; 1nM ARC-1182; 1 μM ARC-904 | 0.39 (0.066) | 5.99 | 0.58 | 8.70 | 5.7 | 14.15 | 2 | 4.00 | 20 | 12.04 | 16.50 | 61.38 |
| 0.1 nM PKAc; 0.5 nM ARC-1182; 1 μM ARC-904 | 0.310 (0.036) | 17.33 | 0.82 | 12.35 | 4.8 | 14.29 | 3 | 3.50 | 4.2 | 14.38 | 18.00 | 79.84 |
| 0.1 nM PKAc; 0.1 nM ARC-1182; 1 μM ARC-904 | 0.313 (0.042) | 16.94 | 0.71 | 10.68 | 6.2 | 14.08 | 4 | 3.00 | 23 | 11.52 | 19.20 | 75.42 |
| 1nM PKAc; 1 nM ARC-1182; 4 μM ARC-904 | 0.35 (0.060) | 11.24 | 0.79 | 11.82 | 4.4 | 14.34 | 0 | 5.0 | 29 | 10.59 | 13.80 | 66.79 |
| 1nM PKAc; 0.5 nM ARC-1182; 4 μM ARC-904 | 0.179 (0.010) | 24.65 | 0.81 | 12.08 | 2.8 | 14.58 | 0 | 5.0 | 10 | 13.48 | 15.30 | 85.09 |
| 1nM PKAc; 0.1 nM ARC-1182; 4 μM ARC-904 | 0.133 (0.005) | 18.32 | 0.85 | 12.75 | 4.8 | 14.28 | 0 | 5.0 | 6.0 | 14.10 | 16.50 | 80.95 |

| | | | | | | | | | | | | |
|---|---|---|---|---|---|---|---|---|---|---|---|---|
| 0.5 nM PKAc; 1nM ARC-1182; 4 µM ARC-904 | 0.252 (0.016) | 25.29 | 0.85 | 12.68 | 4.6 | 14.31 | 2 | 4.0 | 11 | 13.37 | 14.80 | 84.44 |
| 0.5 nM PKAc; 0.5 nM ARC-1182; 4 µM ARC-904 | 0.375 (0.016) | 8.35 | 0.79 | 11.91 | 3.5 | 14.48 | 0 | 5.0 | 7.6 | 13.86 | 16.30 | 69.90 |
| 0.5 nM PKAc; 0.1 nM ARC-1182; 4 µM ARC-904 | 0.228 (0.011) | 28.60 | 0.76 | 11.40 | 6.7 | 13.99 | 2 | 4.0 | 8.6 | 13.71 | 17.50 | 89.19 |
| 0.1 nM PKAc; 1nM ARC-1182; 4 µM ARC-904 | 0.281 (0.029) | 21.30 | 0.72 | 10.80 | 6.2 | 14.08 | 1 | 4.5 | 18 | 12.31 | 15.50 | 78.58 |
| 0.1 nM PKAc; 0.5 nM ARC-1182; 4 µM ARC-904 | 0.195 (0.023) | 26.86 | 0.77 | 11.58 | 10.4 | 13.44 | 0 | 5.0 | 20 | 11.99 | 17.10 | 85.97 |
| 0.1 nM PKAc; 0.1 nM ARC-1182; 4 µM ARC-904 | 0.29 (0.069) | 20.06 | 0.76 | 11.36 | 15.6 | 12.65 | 1 | 4.5 | 41 | 8.78 | 18.30 | 75.64 |
| 1nM PKAc; 1 nM ARC-1182; 8 µM ARC-904 | 0.238 (0.007) | 27.22 | 0.75 | 11.30 | 1.7 | 14.75 | 0 | 5.0 | 5.5 | 14.18 | 12.60 | 85.04 |
| 1nM PKAc; 0.5 nM ARC-1182; 8 µM ARC-904 | 0.234 (0.024) | 27.77 | 0.86 | 12.93 | 8.4 | 13.75 | 0 | 5.0 | 18 | 12.33 | 14.10 | 85.88 |
| 1nM PKAc; 0.1 nM ARC-1182; 8 µM ARC-904 | 0.130 (0.016) | 17.91 | 0.86 | 12.90 | 3.6 | 14.46 | 0 | 5.0 | 21 | 11.89 | 15.30 | 77.45 |
| 0.5 nM PKAc; 1nM ARC-1182; 8 µM ARC-904 | 0.138 (0.011) | 19.01 | 0.75 | 11.25 | 3.0 | 14.56 | 0 | 5.0 | 13 | 13.02 | 13.60 | 76.43 |
| 0.5 nM PKAc; 0.5 nM ARC-1182; 8 µM ARC-904 | 0.159 (0.016) | 21.90 | 0.82 | 12.26 | 3.2 | 14.52 | 0 | 5.0 | 18 | 12.33 | 15.10 | 81.11 |
| 0.5 nM PKAc; 0.1 nM ARC-1182; 8 µM ARC-904 | 0.221 (0.031) | 29.56 | 0.76 | 11.39 | 3.8 | 14.43 | 0 | 5.0 | 24 | 11.36 | 16.30 | 88.03 |
| 0.1 nM PKAc; 1nM ARC- | 0.198 (0.016) | 27.27 | 0.83 | 12.42 | 3.6 | 14.46 | 0 | 5.0 | 14 | 12.88 | 14.40 | 86.42 |

| | | | | | | | | | | | | |
|---|---|---|---|---|---|---|---|---|---|---|---|---|
| 1182; 8 µM ARC-904 | | | | | | | | | | | | |
| 0.1 nM PKAc; 0.5 nM ARC-1182; 8 µM ARC-904 | 0.185 (0.014) | 25.48 | 0.77 | 11.58 | 4.2 | 14.37 | 0 | 5.0 | 13 | 13.03 | 15.90 | 85.36 |
| 0.1 nM PKAc; 0.1 nM ARC-1182; 8 µM ARC-904 | 0.148 (0.018) | 20.39 | 0.80 | 12.00 | 5.6 | 14.16 | 1 | 4.5 | 21 | 11.89 | 17.10 | 85.04 |

## **Appendix 6.** The Estimation of Optimal Conditions for ARC-1411

| Assay conditions | $K_d$ ($SD_{mean}$); (nM) | Weight score of relative bias | Z-factor | Weight score | Relative SD of data points(%) | Weight score | Outlier | Weight score | Relative SD of $K_d$ (%) | Weight score | Economic Weight score | Total score |
|---|---|---|---|---|---|---|---|---|---|---|---|---|
| 1nM PKAc; 80 nM ARC-1182; 5 μM ARC-1411 | 0.0045 (0.0003) | 15.89 | 0.69 | 10.39 | 2.4 | 14.64 | 0 | 5.0 | 12.9 | 13.07 | 10.08 | 69.07 |
| 1nM PKAc; 40 nM ARC-1182; 5 μM ARC-1411 | 0.0036 (0.0003) | 12.86 | 0.88 | 13.17 | 2.6 | 14.61 | 0 | 5.0 | 15.6 | 12.65 | 14.88 | 73.17 |
| 1nM PKAc; 10 nM ARC-1182; 5 μM ARC-1411 | 0.0049 (0.0011) | 17.28 | 0.90 | 13.53 | 6.5 | 14.03 | 1 | 4.5 | 39.8 | 9.03 | 18.48 | 76.85 |
| 0.5 nM PKAc; 80nM ARC-1182; 5 μM ARC-1411 | 0.0066 (0.0012) | 23.51 | 0.65 | 9.73 | 5.0 | 14.25 | 3 | 3.5 | 31.0 | 10.36 | 10.12 | 71.46 |
| 0.5 nM PKAc; 40 nM ARC-1182; 5 μM ARC-1411 | 0.0046 (0.0005) | 16.53 | 0.64 | 9.53 | 2.5 | 14.63 | 2 | 4.0 | 20.1 | 11.98 | 14.92 | 71.59 |
| 0.5 nM PKAc; 10 nM ARC-1182; 5 μM ARC-1411 | 0.0043 (0.0002) | 15.43 | 0.88 | 13.20 | 3.1 | 14.54 | 1 | 4.5 | 8.5 | 13.73 | 18.52 | 79.91 |
| 0.1 nM PKAc; 80nM ARC-1182; 5 μM ARC-1411 | 0.0245 (0.0128) | -27.43 | 0.40 | 5.93 | 2.4 | 14.63 | 7 | 1.5 | 90.2 | 1.47 | 10.15 | 6.26 |
| 0.1 nM PKAc; 40 nM ARC-1182; 5 μM ARC-1411 | 0.0086 (0.0016) | 29.29 | 0.52 | 7.81 | 1.7 | 14.75 | 6 | 2.0 | 32.8 | 10.09 | 14.95 | 78.89 |
| 0.1 nM PKAc; 10 nM ARC-1182; 5 μM ARC-1411 | 0.0069 (0.0008) | 24.58 | 0.55 | 8.25 | 3.5 | 14.47 | 2 | 4.0 | 20.2 | 11.97 | 18.55 | 81.81 |
| 1nM PKAc; 80 nM ARC-1182; 20 μM ARC-1411 | 0.0066 (0.0003) | 23.51 | 0.88 | 13.17 | 3.6 | 14.47 | 0 | 5.0 | 7.8 | 13.82 | 9.84 | 79.82 |
| 1nM PKAc; 40 nM ARC-1182; 20 μM ARC-1411 | 0.0076 (0.0011) | 27.08 | 0.83 | 12.47 | 10.8 | 13.38 | 2 | 4.0 | 25.3 | 11.21 | 14.64 | 82.77 |
| 1nM PKAc; 10 nM ARC-1182; 20 μM ARC-1411 | 0.022 (0.0018) | -17.20 | 0.92 | 13.82 | 7.6 | 13.86 | 0 | 5.0 | 14.7 | 12.80 | 18.24 | 46.52 |
| 0.5 nM PKAc; 80nM ARC-1182; 20 μM ARC-1411 | 0.0061 (0.0006) | 21.73 | 0.75 | 11.28 | 3.3 | 14.50 | 1 | 4.5 | 16.7 | 12.50 | 9.88 | 74.39 |
| | | | | | | | | | | | | |

| | | | | | | | | | | | | |
|---|---|---|---|---|---|---|---|---|---|---|---|---|
| 0.5 nM PKAc; 40 nM ARC-1182; 20 µM ARC-1411 | 0.011 (0.0006) | 19.21 | 0.79 | 11.79 | 3.9 | 14.42 | 0 | 5.0 | 9.3 | 13.61 | 14.68 | 78.71 |
| 0.5 nM PKAc; 10 nM ARC-1182; 20 µM ARC-1411 | 0.0078 (0.0007) | 27.79 | 0.80 | 12.05 | 9.6 | 13.56 | 0 | 5.0 | 16.1 | 12.59 | 18.28 | 89.26 |
| 0.1 nM PKAc; 40 nM ARC-1182; 20 µM ARC-1411 | 0.0085 (0.0015) | 29.68 | 0.42 | 6.28 | 4.9 | 14.27 | 5 | 2.5 | 29.8 | 10.53 | 14.71 | 77.97 |
| 0.1 nM PKAc; 10 nM ARC-1182; 20 µM ARC-1411 | 0.010 (0.0018) | 23.59 | 0.75 | 11.18 | 6.1 | 14.08 | 5 | 2.5 | 29.8 | 10.53 | 18.31 | 80.19 |
| 1nM PKAc; 80 nM ARC-1182; 40 µM ARC-1411 | 0.0096 (0.0011) | 25.69 | 0.60 | 8.94 | 2.7 | 14.59 | 0 | 5.0 | 20.1 | 11.98 | 9.36 | 75.57 |
| 1nM PKAc; 40 nM ARC-1182; 40 µM ARC-1411 | 0.0041 (0.0006) | 14.54 | 0.85 | 12.70 | 3.0 | 14.55 | 0 | 5.0 | 23.5 | 11.48 | 14.16 | 72.42 |
| 1nM PKAc; 10 nM ARC-1182; 40 µM ARC-1411 | 0.0043 (0.0005) | 15.43 | 0.93 | 13.90 | 5.1 | 14.24 | 0 | 5.0 | 19.0 | 12.15 | 17.76 | 78.48 |
| 0.5 nM PKAc; 80nM ARC-1182; 40 µM ARC-1411 | 0.0111 (0.0012) | 20.31 | 0.64 | 9.55 | 4.0 | 14.40 | 6 | 2.0 | 18.8 | 12.18 | 9.40 | 67.83 |
| 0.5 nM PKAc; 40 nM ARC-1182; 40 µM ARC-1411 | 0.0027 (0.0002) | 9.51 | 0.71 | 10.64 | 7.3 | 13.91 | 1 | 4.5 | 14.1 | 12.89 | 14.20 | 65.65 |
| 0.5 nM PKAc; 10 nM ARC-1182; 40 µM ARC-1411 | 0.0015 (0.00001) | 5.31 | 0.79 | 11.92 | 13.8 | 12.93 | 0 | 5.0 | 1.4 | 14.79 | 17.80 | 67.74 |
| 1nM PKAc; 80 nM ARC-1182; 80 µM ARC-1411 | 0.01142 (0.0013) | 19.31 | 0.86 | 12.91 | 2.8 | 14.59 | 1 | 4.5 | 19.7 | 12.04 | 9.36 | 72.72 |
| 1nM PKAc; 40 nM ARC-1182; 80 µM ARC-1411 | 0.01249 (0.0008) | 15.50 | 0.82 | 12.28 | 3.6 | 14.46 | 0 | 5.0 | 10.6 | 13.42 | 14.16 | 74.82 |
| 1nM PKAc; 10 nM ARC-1182; 80 µM ARC-1411 | 0.01174 (0.0006) | 18.17 | 0.84 | 12.65 | 5.1 | 14.24 | 0 | 5.0 | 9.0 | 13.65 | 17.76 | 81.48 |
| 0.5 nM PKAc; 80nM ARC-1182; 80 µM ARC-1411 | 0.01154 (0.0013) | 18.89 | 0.77 | 11.52 | 3.4 | 14.49 | 0 | 5.0 | 19.8 | 12.03 | 9.40 | 71.33 |
| 0.5 nM PKAc; 40 nM ARC-1182; 80 µM ARC-1411 | 0.00743 (0.0013) | 26.47 | 0.74 | 11.04 | 4.1 | 14.39 | 2 | 4.0 | 31.2 | 10.32 | 14.20 | 80.43 |
| | | | | | | | | | | | | |

| | | | | | | | | | | | | |
|---|---|---|---|---|---|---|---|---|---|---|---|---|
| 0.5 nM PKAc; 10 nM ARC-1182; 80 µM ARC-1411 | 0.00812 (0.0021) | 28.93 | 0.85 | 12.68 | 10.0 | 13.50 | 0 | 5.0 | 44.2 | 8.37 | 17.80 | 86.27 |
| 0.1 nM PKAc; 10 nM ARC-1182; 80 µM ARC-1411 | 0.1087 (0.0023) | 21.27 | 0.66 | 9.94 | 4.1 | 14.38 | 0 | 5.0 | 36.1 | 9.59 | 17.83 | 78.01 |